Library copy
R.A. 1242

[redacted]

RM No. L7D09

Restriction/Classification Cancelled

NACA

APR 16 1947

RESEARCH MEMORANDUM

for the

Air Materiel Command, Army Air Forces

AIR-STREAM SURVEYS IN THE VICINITY OF THE TAIL OF A 1/8.33-SCALE POWERED MODEL OF THE REPUBLIC XF-12 AIRPLANE

By

Gerald V. Foster

Langley Memorial Aeronautical Laboratory
Langley Field, Va.

Restriction/Classification Cancelled

NATIONAL ADVISORY COMMITTEE FOR AERONAUTICS

WASHINGTON

APR 8 1947

NACA RM No. L7D09

NATIONAL ADVISORY COMMITTEE FOR AERONAUTICS

RESEARCH MEMORANDUM

for the

Air Materiel Command, Army Air Forces

AIR-STREAM SURVEYS IN THE VICINITY OF THE TAIL OF A 1/8.33-SCALE POWERED MODEL OF THE REPUBLIC XF-12 AIRPLANE

By Gerald V. Foster

SUMMARY

The XF-12 airplane was designed by Republic Aviation Corporation to provide the Army Air Forces with a high performance, photo reconnaissance aircraft. A series of air-stream surveys were made in the vicinity of the empennage of a 1/8.33-scale powered model of the XF-12 airplane in the Langley 19-foot pressure tunnel. Surveys of the vertical-tail region were made through a range of yaw angles of ±20° at a high and low angle of attack. The horizontal-tail surveys were made over a fairly wide range of angles of attack at zero degrees yaw. Several power and flap conditions were investigated. The results are presented in the form of dynamic pressure ratios, sidewash angles, and downwash angles plotted against vertical distance from the fuselage center line.

The results of the investigation indicate that a vertical tail located in a conventional position would be in a field of flow where the dynamic pressure ratios are equal to or close to unity except in the vicinity of the fuselage, and that the variation of sidewash angle with angle of yaw was stabilizing. With flaps retracted, power caused the dynamic pressure ratios at the horizontal tail to be increased; for equal lift coefficients, the effect of power or flap deflection on the direction of flow at any particular point in the region of the horizontal tail is small.

INTRODUCTION

A high performance, photo reconnaissance airplane designated the XF-12 was designed and constructed for the Army Air Forces by Republic Aviation Corporation. At the request of the Air Materiel Command, Army Air Forces, an investigation has been conducted in the

Langley 19-foot pressure tunnel to determine some of the aerodynamic characteristics of a 1/8.33-scale powered model of the XF-12 airplane.

The results of the investigations to determine the static lateral and longitudinal stability characteristics are presented in references 1 and 2, respectively; the stalling characteristics are included in reference 2.

In order to obtain information relative to the design of the vertical and horizontal tail surfaces, dynamic pressure, sidewash, and downwash surveys were made in the vicinity of the empennage. The vertical-tail surveys were made through a range of yaw angles of ±20° at a high and a low angle of attack, and data pertinent to the horizontal-tail design were obtained over a fairly wide range of angles of attack for the unyawed condition. Several power and flap conditions were investigated.

COEFFICIENTS AND SYMBOLS

The coefficients and symbols used are defined as follows:

C_L lift coefficient (L/qS)

T_c effective thrust coefficient $(T/2qD^2)$

Q_c torque coefficient $(Q/2qD^3)$

L lift (-Z)

q free-stream dynamic pressure $\left(\frac{1}{2}\rho V^2\right)$

ρ mass density of air

μ coefficient of viscosity of air

V free-stream velocity

T effective thrust of one propeller

D propeller diameter

Q torque of one propeller

α angle of attack of wing root chord line

ψ angle of yaw

δ_f flap deflection

S wing area

q_t local dynamic-pressure at tail

q_t/q dynamic-pressure ratio at tail

ϵ local downwash angle at tail, positive when velocity component normal to direction of free-stream velocity is downward

σ local sidewash angle at tail, positive when horizontal velocity component is to left, viewed from rear of airplane

S_t area of horizontal tail of model (projected)

b_t span of horizontal tail of model (projected)

c_t local chord of horizontal tail

MODEL AND APPARATUS

The 1/8.33-scale powered model of the XF-12 airplane is shown mounted on the single support in the Langley 19-foot pressure tunnel in figure 1. A three-view drawing of the model is presented in figure 2, and a complete description of the model and its components are given in references 1 and 2. The horizontal and vertical tail and after portion of the fuselage were replaced by a fuselage tail cone during this part of the investigation.

The Langley 19-foot pressure tunnel air-stream rake was employed to measure dynamic pressures, downwash angles, and sidewash angles. The rake, which had been previously calibrated through a known pitch and yaw range, consists of six pitot-static tubes with pitch and yaw orifices (two each) drilled in the hemispherical tips at 45° to the longitudinal tube axes and 90° to each other. The tubes, which are alined in vertical plane and are spaced 3 inches apart (fig. 3), were connected to a multiple tube manometer. The manometer readings were recorded during the tests by means of a camera. The mechanism of the survey-strut carriage allowed only planes to be traversed that were perpendicular to the longitudinal axis of the tunnel.

TEST CONDITIONS AND METHODS

The air-stream survey tests were conducted at a value of dynamic pressure of 26.7 pounds per square foot with the density of the air in the tunnel maintained at approximately 0.00525 slug per cubic foot. These conditions correspond to a Reynolds number and Mach number of about 2,260,000 and 0.09, respectively.

The methods of duplicating power for the vertical and horizontal tail surveys were the same as reported in references 1 and 2, respectively. The variation of T_c with C_L for the power conditions simulated for sea level operation are presented in figure 4. A comparison of the variation of Q_c with T_c is given in figure 5 for the full-scale variable-pitch propeller and the model adjustable fixed-pitch propeller. The full-scale power conditions simulated are listed in table I.

Air-stream surveys at the vertical tail.- The nature of the flow in the vicinity of the vertical tail was investigated through a range of yaw angles of $\pm 20^{\circ}$ at angles of attack of approximately 2° and 11° for several model and power conditions.

The survey rake was located in the vicinity of a line corresponding to the rudder hinge line. Inasmuch as the distance between a plane of survey and a reference point corresponding to the midpoint of the rudder span along the rudder hinge line changed as the angle of attack and angle of yaw were changed, three longitudinal positions of the survey apparatus were selected so that the plane of survey was within ± 1.0 inch of the reference point (fig. 6). Two vertical settings of the survey rake were made 18 inches apart, in order to cover the span of the tail.

Air-stream surveys at the horizontal tail.- Air-stream survey measurements were made through a range of angles of attack ($\psi = 0^{\circ}$) for several power and flap conditions.

The flow was investigated at 11 spanwise locations in a plane perpendicular to the plane of symmetry of the model and passing through a point near the 1/4-chord point of the mean aerodynamic chord (M.A.C.) of the horizontal tail. As it was not practical to change the longitudinal position of the survey apparatus during tests in order to maintain the same relative position with respect to the model, a position was selected such that the maximum movement of the 1/4-chord point of the mean aerodynamic chord was 0.4 inch or less from the plane of survey. Two vertical settings of the rake were made at each spanwise location so that measurements were spaced 1.5 inches (fig. 7).

RESULTS AND DISCUSSION

Jet-boundary corrections were applied to the survey data obtained at the horizontal tail. These corrections consist of an angle change to the downwash angles and a downward displacement of the field of flow. No corrections have been applied to the vertical-tail survey data. The wing angles of attack have been corrected for jet-boundary effects and air-stream misalinement, and the lift coefficients have been corrected for model support-strut interference.

Air-stream surveys at the vertical tail.- The tail-off lift characteristics are presented in figure 8 and the results of the surveys are presented as indicated in the following table:

Figure	δ_f (deg)	Power	Landing gear	α (deg)
9(a)	0	Propeller removed	Off	2.1
9(b)	↓	↓	↓	10.9
9(c)	↓	$T_c = 0$	↓	2.1
9(d)	↓	↓	↓	10.9
9(e)	↓	$(M.P.)_2$	↓	2.1
9(f)	↓	↓	↓	11.1
10(a)	55	Propellers removed	On	2.0
10(b)	↓	↓	↓	11.3
10(c)	↓	$T_c = 0$	↓	2.0
10(d)	↓	↓	↓	11.4
10(e)	↓	0.50(R.P.)	↓	2.2
10(f)	↓	↓	↓	11.8

The results of the surveys indicate that a vertical tail located in a conventional position would be in a field of flow where the dynamic pressure ratios are equal to or close to unity except in the vicinity of the fuselage. Although average weighted values of dynamic pressure ratios and sidewash angles have not been calculated, the data indicate that a stabilizing variation of sidewash angle with angle of yaw was obtained for the conditions tested.

Air-stream surveys at the horizontal tail.- The tail-off lift characteristics are presented in figure 11, and the results of the surveys are presented as indicated in the following table:

Figure	Type	δ_f (deg)	Power	Landing gear	α (deg)
12(a)	q_t/q	0	Propellers removed	Off	0.2,3.4,6.5,9.6,12.9
12(b)			$T_c = 0$		0.2,3.4,6.5,9.7,12.9
12(c)			0.75(R.P.)		0.2,3.5,6.6,9.8,13.1
13(a)	ϵ	0	Propellers removed	Off	0.2,3.4,6.5,9.6,12.9
13(b)			$T_c = 0$		0.2,3.4,6.5,9.7,12.9
13(c)			0.75(R.P.)		0.2,3.5,6.6,9.8,13.1
14(a)	q_t/q	40	Propellers removed	On	0.9,4.0,7.3,10.4,13.3
14(b)			$T_c = 0$		0.8,4.0,7.2,10.5,13.6
14(c)			0.50(R.P.)		0.9,4.2,7.5,10.9,14.1
15(a)	ϵ	40	Propellers removed	On	0.9,4.0,7.3,10.4,13.3
15(b)			$T_c = 0$		0.8,4.0,7.2,10.5,13.6
15(c)			0.50(R.P.)		0.9,4.2,7.5,10.9,14.1

The dynamic pressure ratios near the tail appear to be reduced with propellers operating at $T_c = 0$ (figs. 12(a) and 12(b)). As would be expected with flaps retracted, application of power increased the dynamic pressure ratios in the vicinity of the horizontal tail (figs. 12(b) and 12(c)). This is due in part to the increased velocity in the slipstream itself, and in part to the tendency of the propeller operation to clean up the flow over the wing. The effect of flap deflection was to shift the wake center downward.

The results of the downwash surveys indicate that for a given lift coefficient the effect of power and flap deflection on the direction of flow at any particular point in the region of the tail plane is small.

Average weighted values of dynamic pressure ratios and downwash angles have been computed for all conditions tested and are presented in table II. The average weighted values were calculated for the vertical location of the horizontal tail shown in figure 7 by means of the following equations:

$$(q_t/q)_{average} = \frac{1}{S_t} \int_{-\frac{b_t}{2}}^{\frac{b_t}{2}} (q_t/q)\, c_t\, db_t$$

and

$$\epsilon_{average} = \frac{1}{S_t(q_t/q)_{average}} \int_{-\frac{b_t}{2}}^{\frac{b_t}{2}} (q_t/q)c_t \epsilon db_t$$

For the given tail location the rate of change of downwash angle with angle of attack varied from 0.38 to 0.41 except for the case of flaps deflected with 0.50(R.P.) where the value was 0.52 (table II).

CONCLUDING REMARKS

Air-stream surveys have been made in the vicinity of the empennage of a 1/8.33-scale powered model of the Republic XF-12 airplane. The results indicate that the vertical tail located in a conventional position would be in a field of flow where the dynamic pressure ratios are equal to or close to unity except in the vicinity of the fuselage, and that the variation of sidewash angle with angle of yaw was stabilizing. With flaps retracted, power caused the dynamic pressure ratios at the horizontal tail to be increased. For equal lift coefficients, the effect of power or flap deflection on the direction of flow at any particular point in the region of the tail plane is small.

Langley Memorial Aeronautical Laboratory
National Advisory Committee for Aeronautics
Langley Field, Va.

Gerald V. Foster
Gerald V. Foster
Aeronautical Engineer

Approved: Clinton H. Dearborn
Clinton H. Dearborn
Chief of Full-Scale Research Division

DBC

REFERENCES

1. Pepper, Edward, and Foster, Gerald V.: Lateral Stability Characteristics of a 1/8.33-Scale Powered Model of the Republic XF-12 Airplane. NACA RM No. L7B21, Army Air Forces, 1947.

2. Pepper, Edward, and Foster, Gerald V.: Longitudinal Stability and Stalling Characteristics of a 1/8.33-Scale Model of the Republic XF∂12 Airplane. NACA RM No. L6L12, Army Air Forces, 1946.

TABLE I

FULL-SCALE POWER CONDITIONS

[Simulated in tests of the 1/8.33-scale model of the XF-12 airplane]

Power condition	Symbol	Brake horsepower (per engine)	Cooling-fan horsepower (per fan)	Airplane gross weight (lb)	Altitude (ft)	Engine speed (rpm)	Gear ratio	Propeller speed (rpm)
Military power	$(M.P.)_2$	3000	54	103,000	0 (sea level)	2700	0.425	1148
75-percent rated power	0.75(R.P.)	1875	20	103,000	0 (sea level)	1500	0.425	638
50-percent rated power	0.50(R.P.)	1250	14	103,000	0 (sea level)	1500	0.425	638
Thrust coefficient equal zero	$T_c = 0$	Low	Low	All weights	All	Low	0.425	Low

NATIONAL ADVISORY
COMMITTEE FOR AERONAUTICS

TABLE II

WEIGHTED AVERAGE VALUES OF q_t/q AND ϵ

δ_f (deg)	Power condition	α (deg)	$q_t/q_{average}$	$\epsilon_{average}$ (deg)	$d\epsilon/d\alpha$
0 ↓	Propellers removed ↓	0.2 3.4 6.5 9.6 12.9	0.98 ↓ .90	1.6 2.7 3.8 5.2 6.3	0.038
	T_c = 0 ↓	0.2 3.4 6.5 9.7 12.9	1.02 .97 .96 .94 .88	1.5 2.6 3.8 5.5 6.4	0.038
	0.75(R.P.) ↓	0.2 3.5 6.6 9.8 13.1	0.97 .95 1.03 1.10 1.16	1.6 2.9 4.2 6.0 6.7	0.041
40 ↓	Propellers removed ↓	0.9 4.0 7.3 10.4	1.00 ↓	5.0 6.7 7.7 8.7	0.041
	T_c = 0 ↓	0.9 4.2 7.5 10.9	1.01 1.01 .99 .93	5.4 6.6 8.1 9.5	0.041
	0.50(R.P.) ↓	0.8 4.0 7.2 10.5 13.6	.99 ↓ 1.06	5.6 7.2 8.8 10.6 12.5	0.052

NATIONAL ADVISORY
COMMITTEE FOR AERONAUTICS

[redacted]

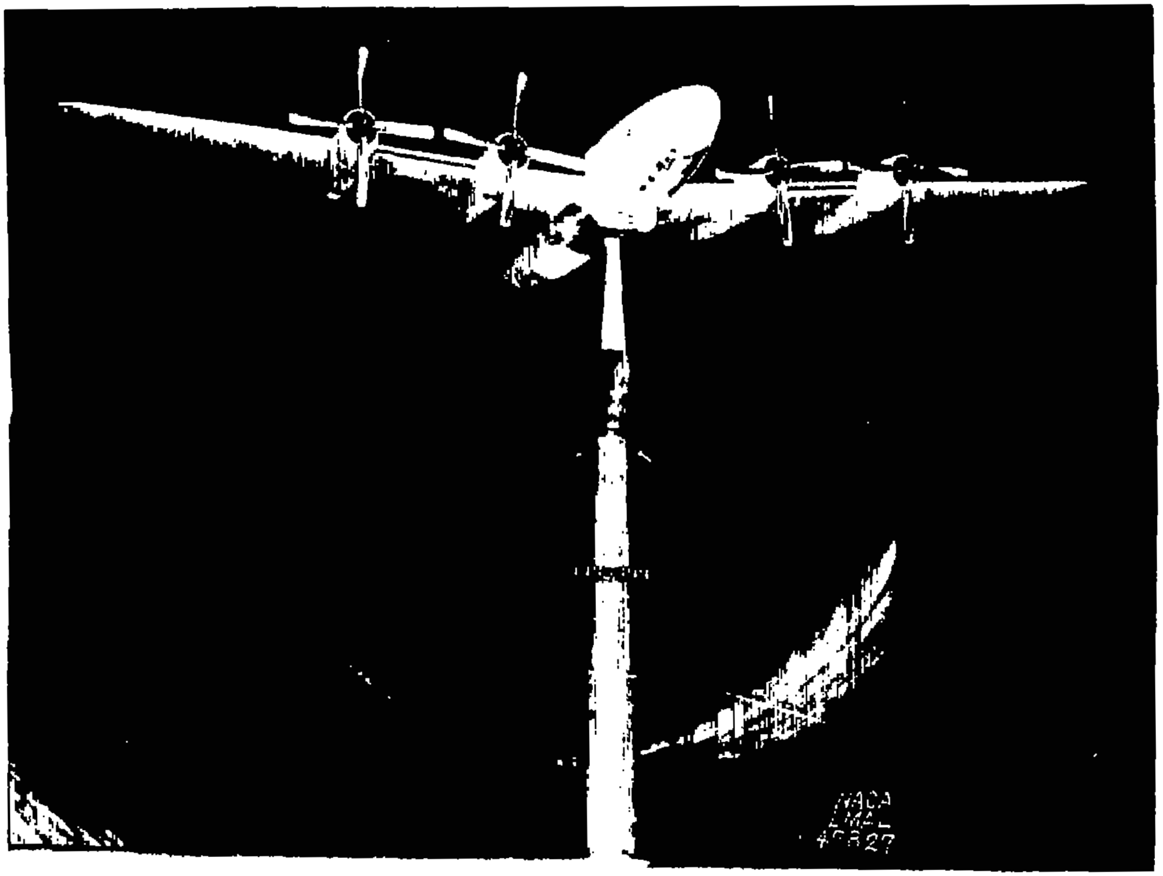

Figure 1.- The $\frac{1}{8.33}$-scale model of the XF-12 airplane mounted in the test section of the Langley 19-foot pressure tunnel.

[redacted]

[redacted]

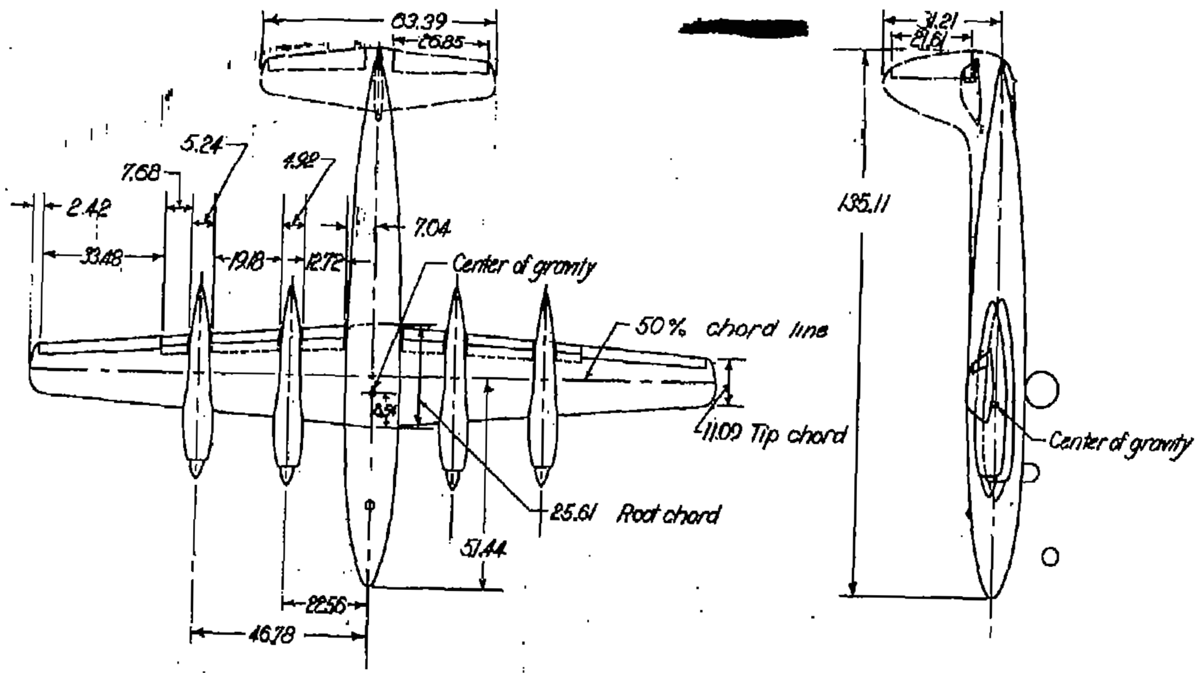

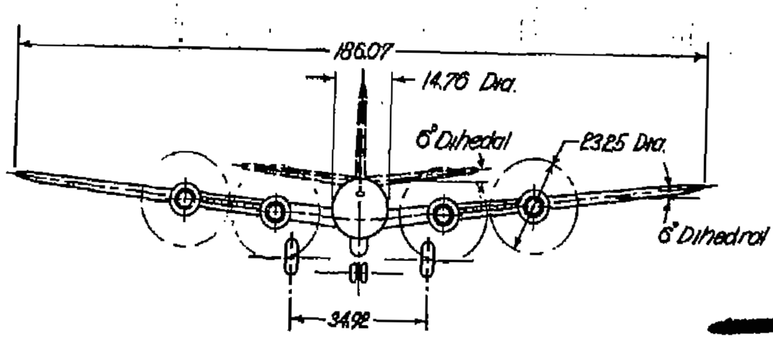

Wing Root Airfoil	R-4,40-318-1
Wing Tip Airfoil	R-4,40-413-.6
Aspect Ratio	10.18
Taper Ratio	2.31 : 1
Wing Incidence	+2° to ¢ of fuselage
Wing Tip Twist (geometric)	-4°
Wing MAC	19.34 in.

Note: All dimensions are given in inches

NATIONAL ADVISORY
COMMITTEE FOR AERONAUTICS

[redacted]

Figure 2 .- Three view drawing of a 1/8.33 - scale model of the Republic XF-12 airplane.

[redacted]

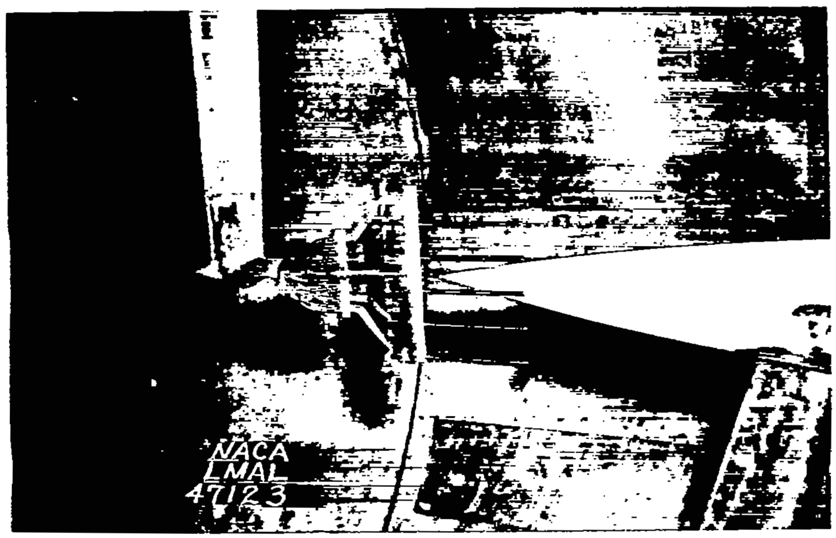

(a) Closeup of rake head.

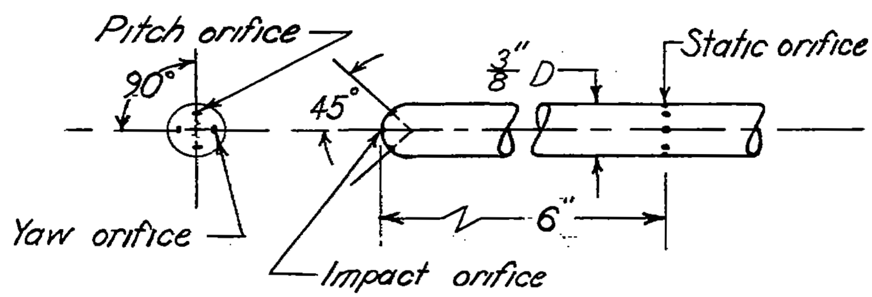

(b) Sketch of tube head.

Figure 3.- Langley 19-foot pressure tunnel air stream survey rake.

NATIONAL ADVISORY COMMITTEE FOR AERONAUTICS
LANGLEY MEMORIAL AERONAUTICAL LABORATORY - LANGLEY FIELD, VA

[redacted]

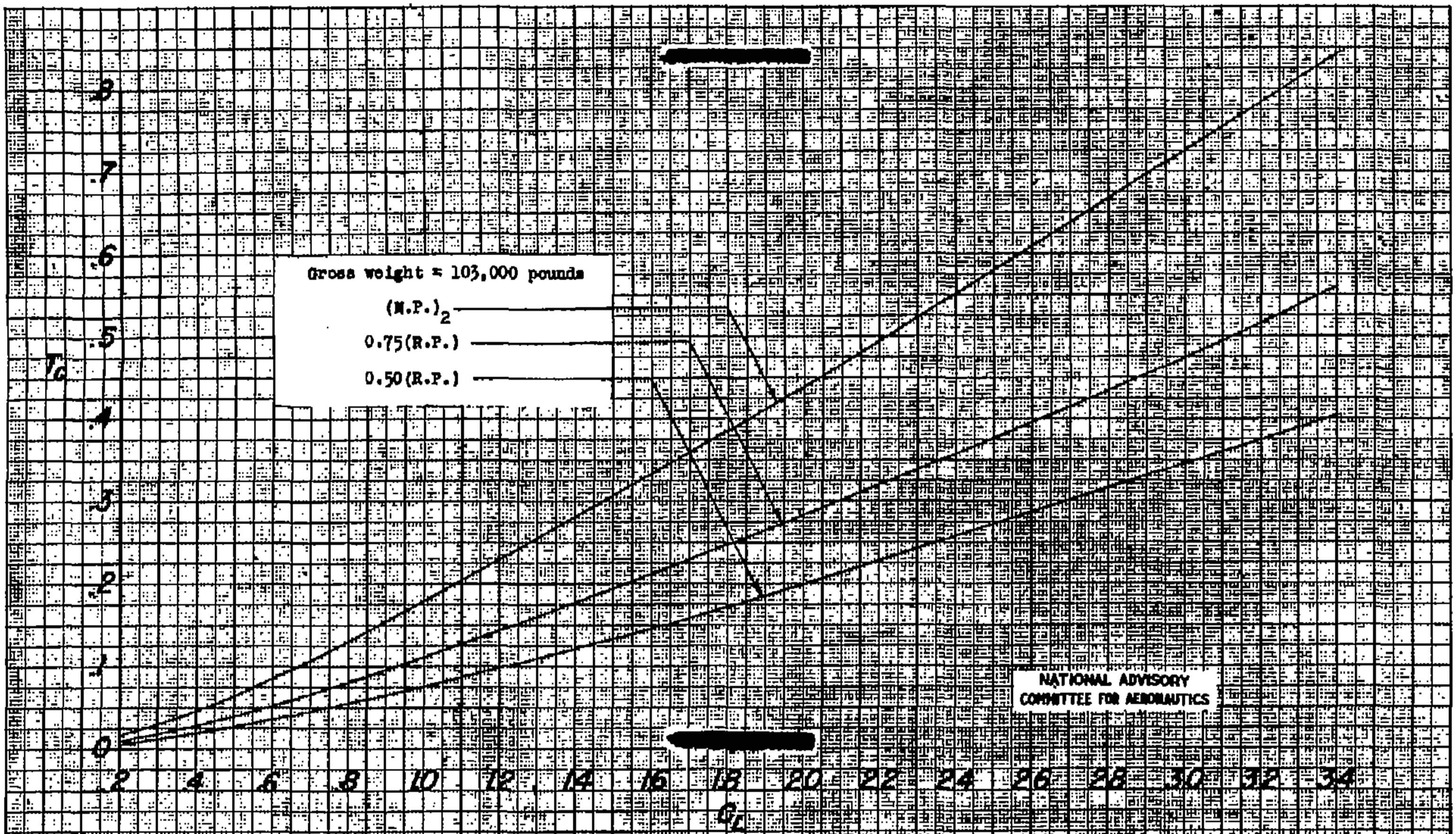

Figure 4.- Variation of thrust coefficient with lift coefficient for several power conditions.

[redacted]

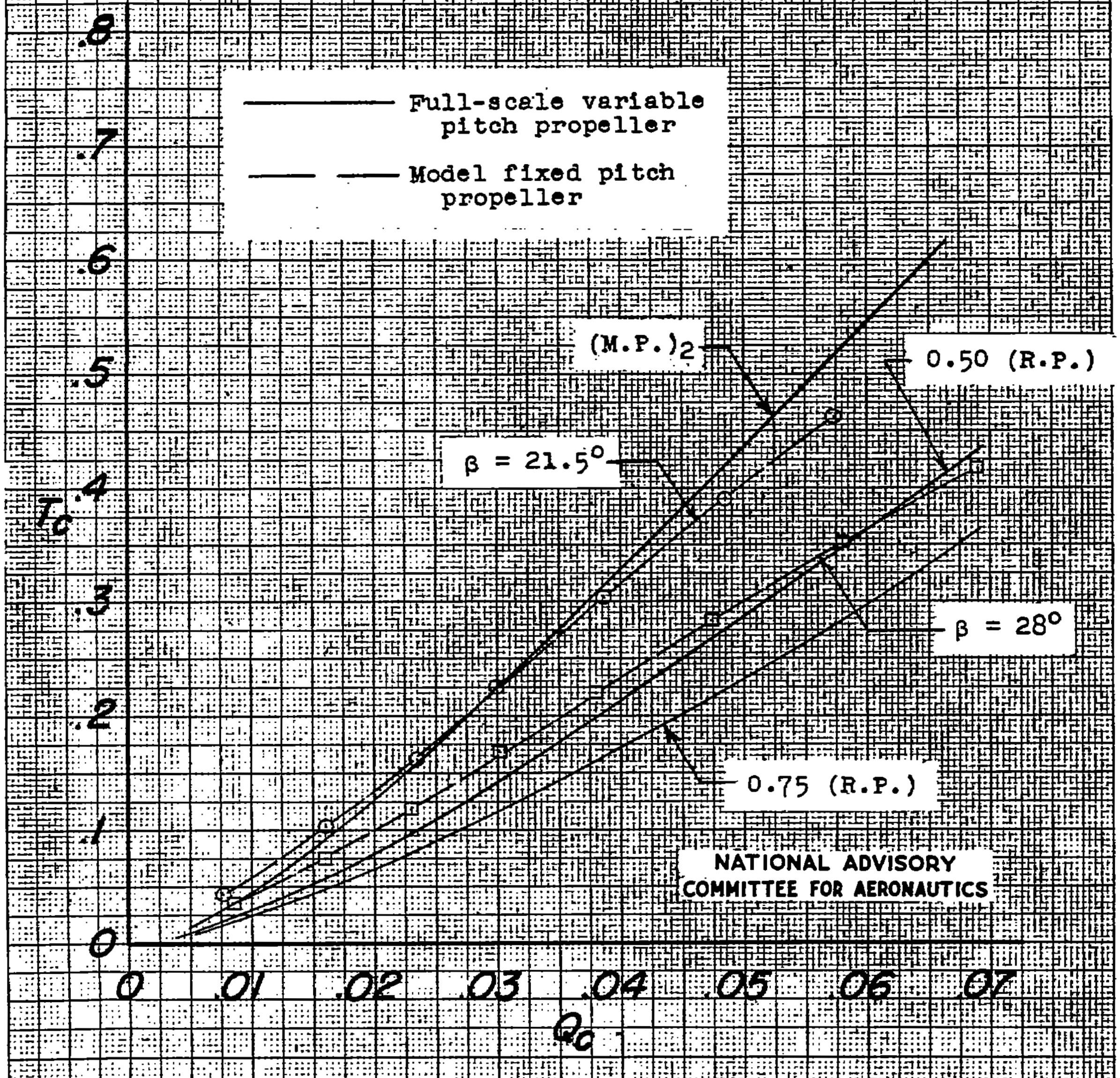

Figure 5.- Variation of thrust coefficient with torque coefficient for sea level operations.

[redacted]

[redacted]

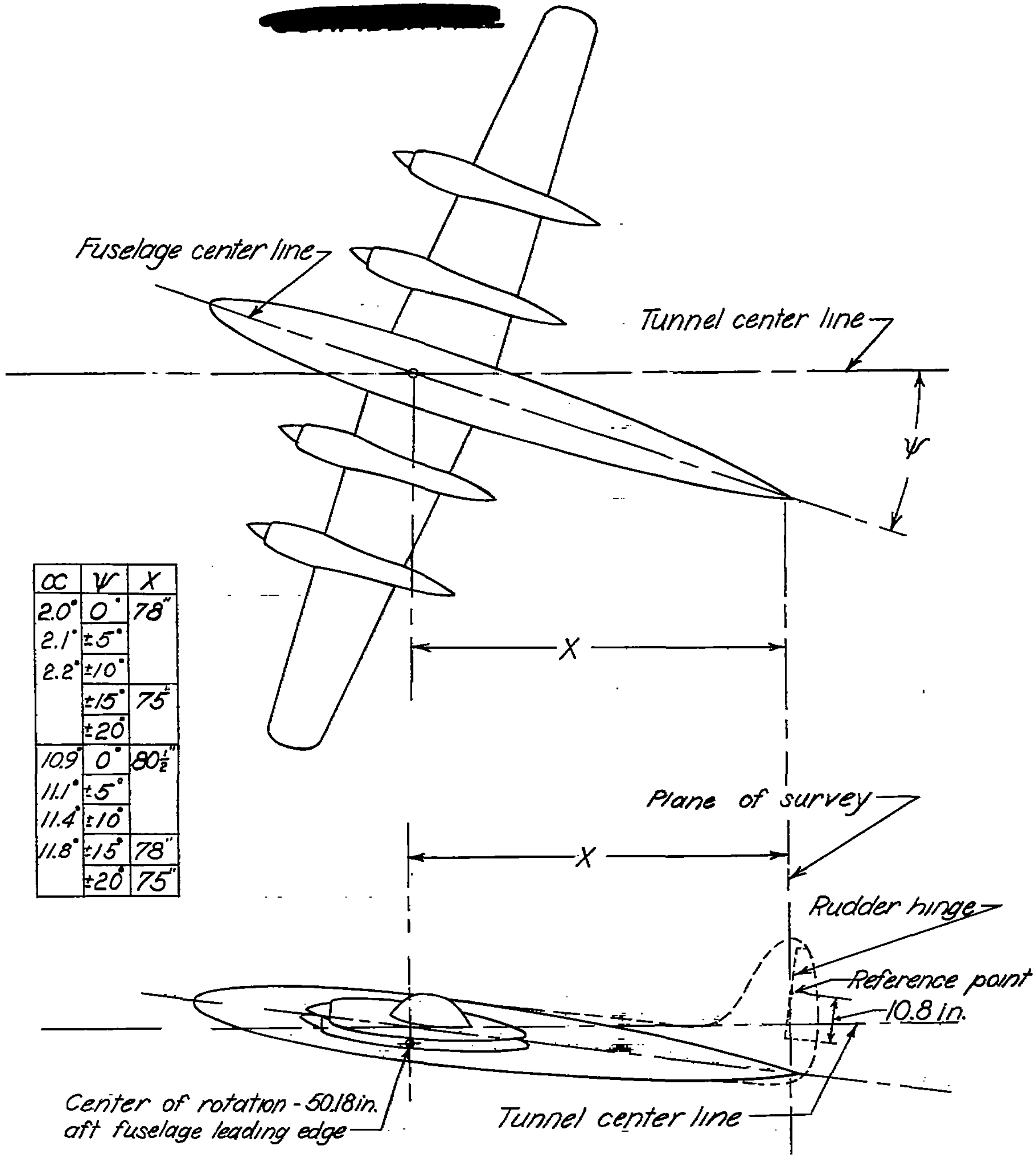

α	ψ	X
2.0°	0°	78"
2.1°	±5°	
2.2°	±10°	
	±15°	75"
	±20°	
10.9°	0°	80½"
11.1°	±5°	
11.4°	±10°	
11.8°	±15°	78"
	±20°	75"

Figure 6.- Arrangement of survey apparatus for measurement of airflow characteristics in vertical tail vicinity.

[redacted]

[redacted]

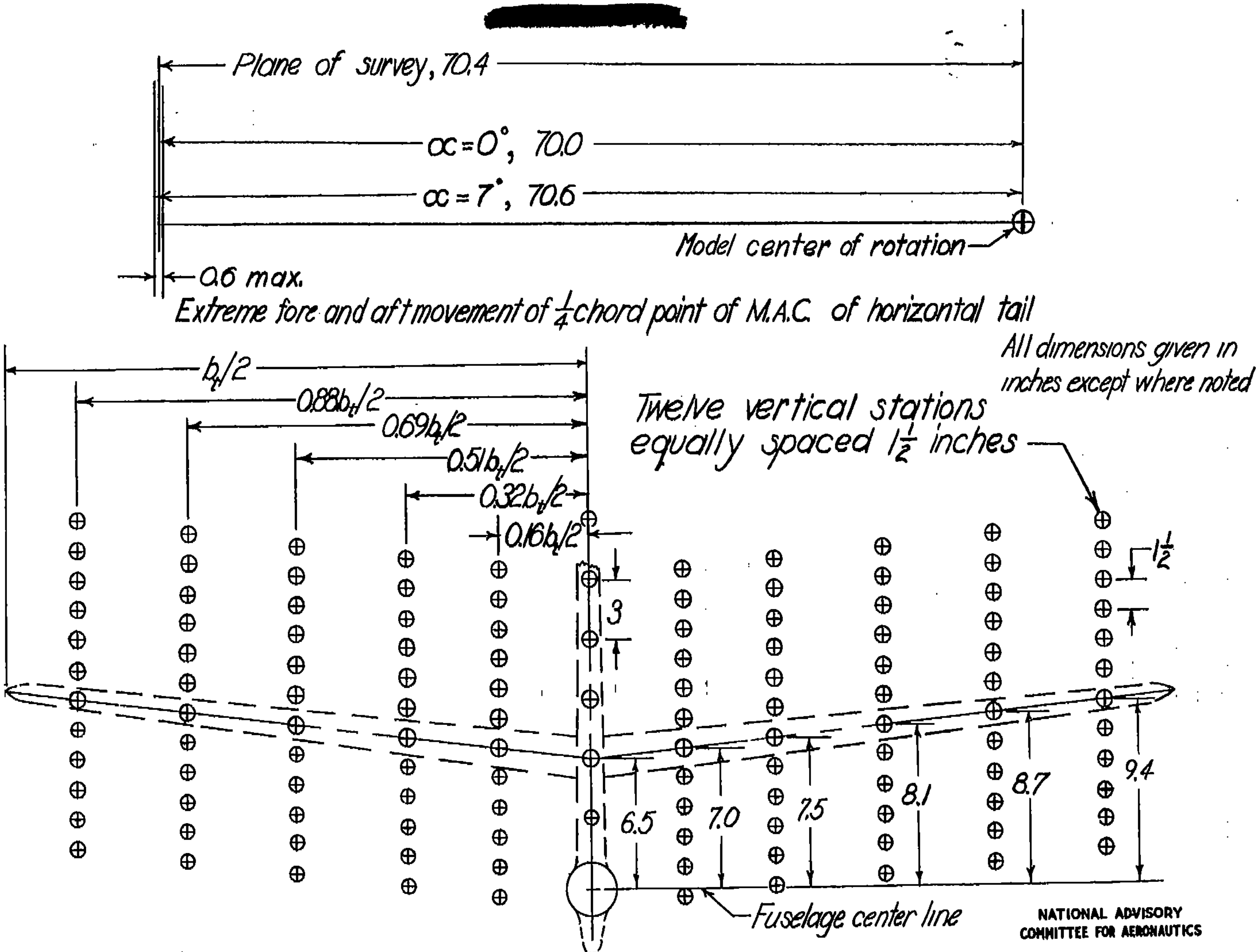

Figure 7.- Airstream survey plane for tests at the horizontal tail of the $\frac{1}{8.33}$-scale model of the Republic XF-12 airplane. [redacted]

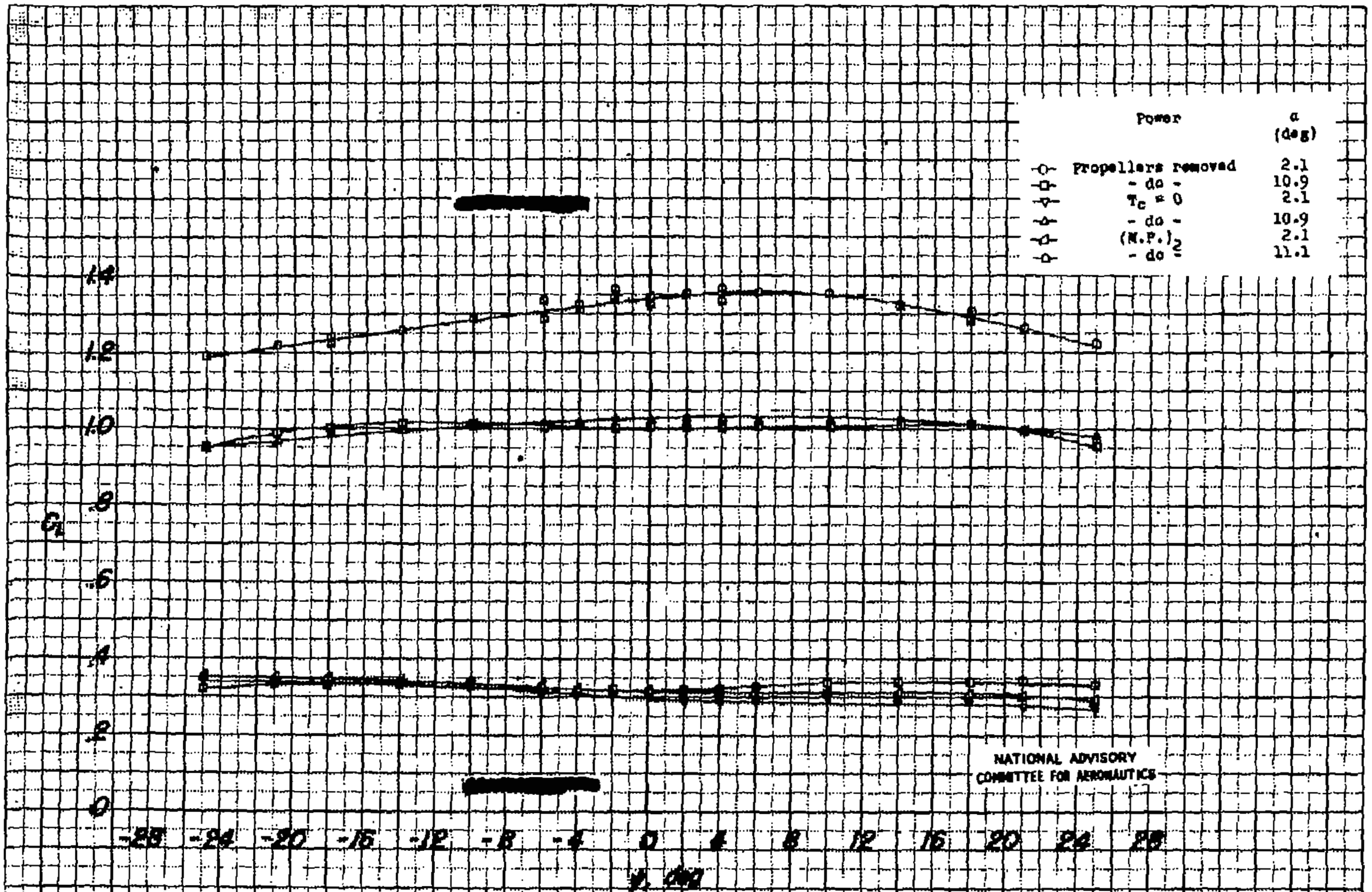

(a) $\delta_f = 0°$

Figure 8.- Variation of lift coefficient with angle of yaw for several power conditions and angles of attack.

2104 8

[redacted]

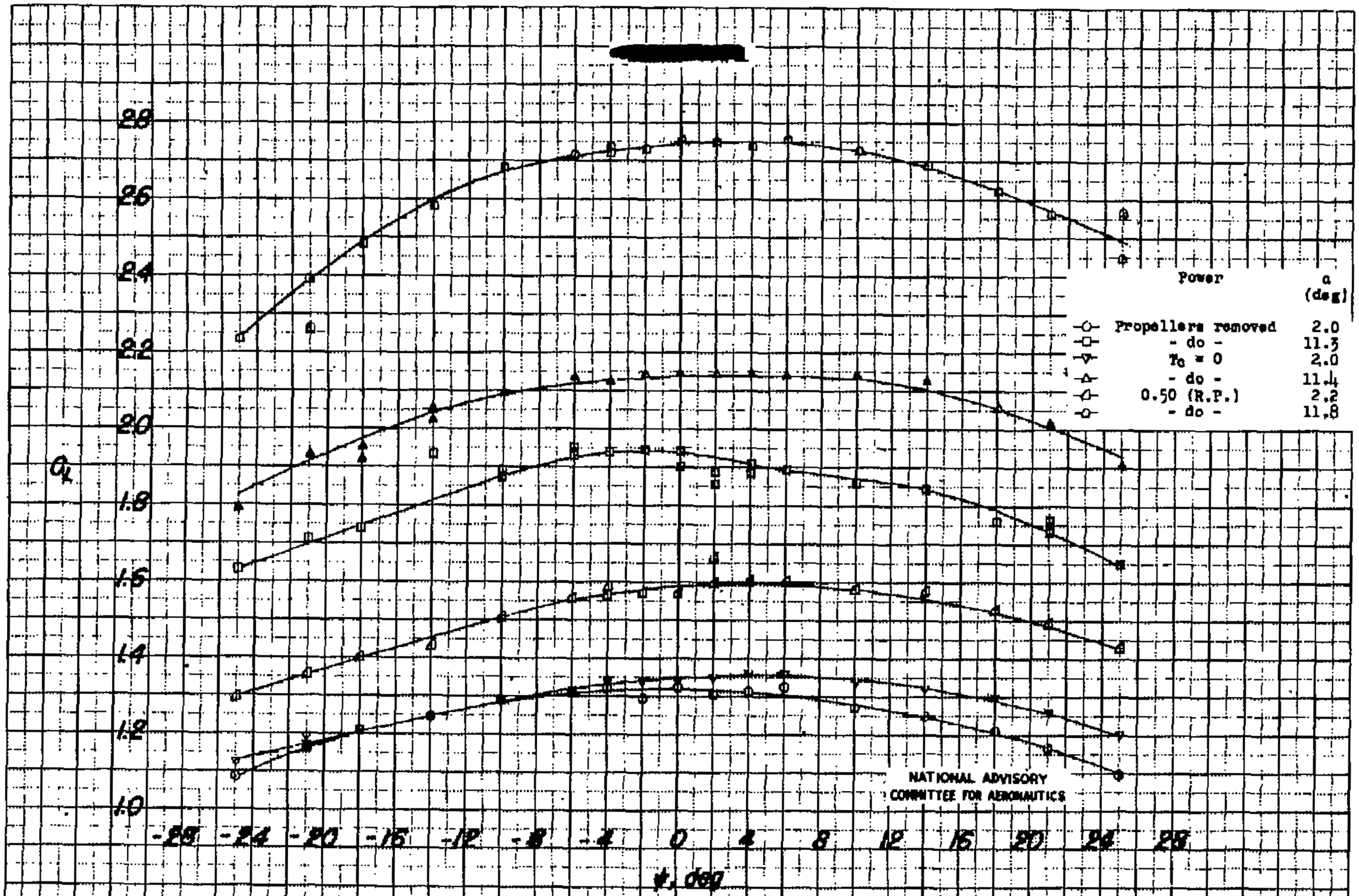

(b) $\delta_f = 55^\circ$

Figure 8 .- Concluded.

[redacted]

[redacted]

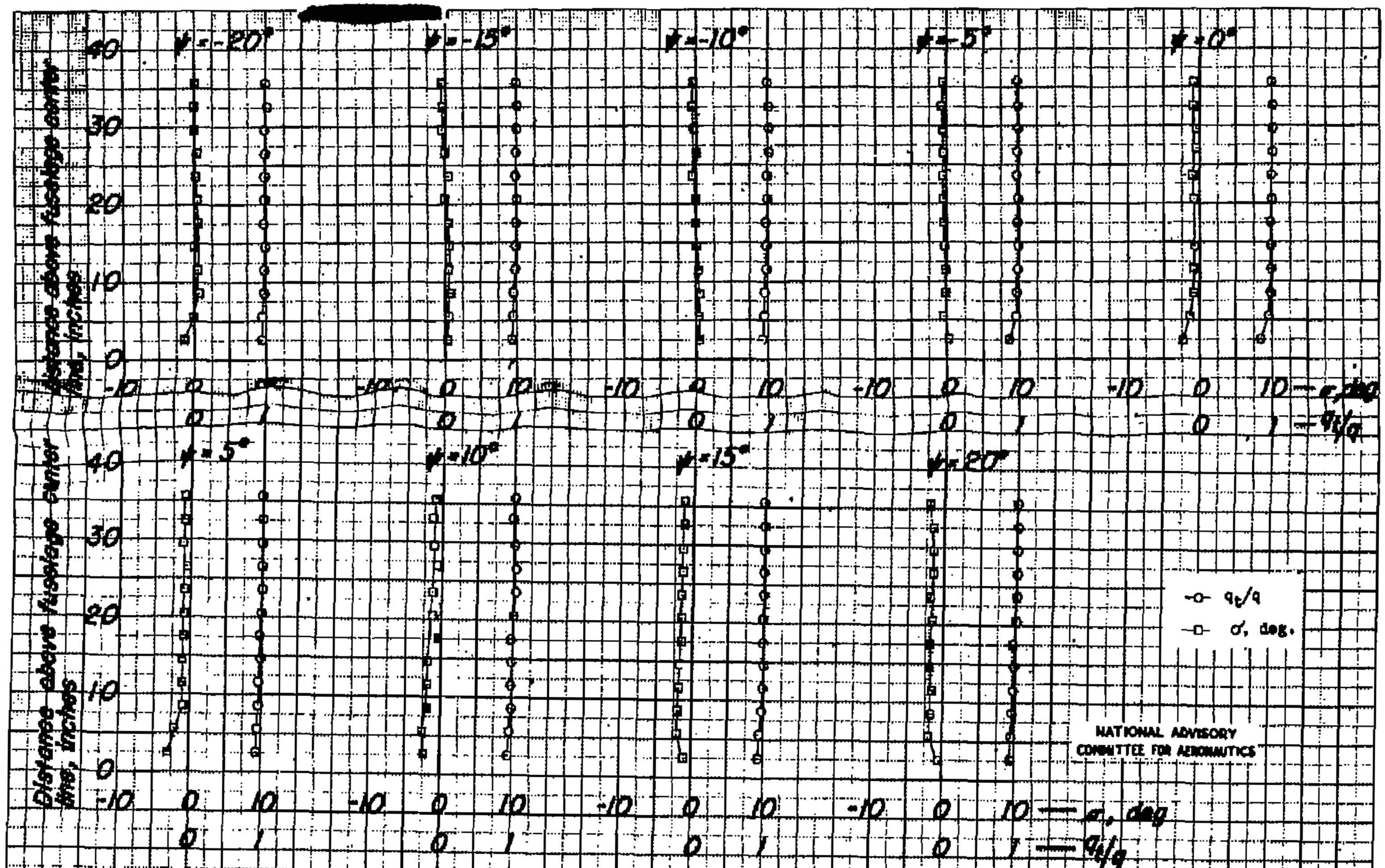

[redacted] (a) Propellers removed; α = 2.1

Figure 9 .- Variation of sidewash angles and dynamic pressure ratios along the span of the vertical tail for various angles of yaw. $\delta_f = 0^{\circ}$.

[redacted]

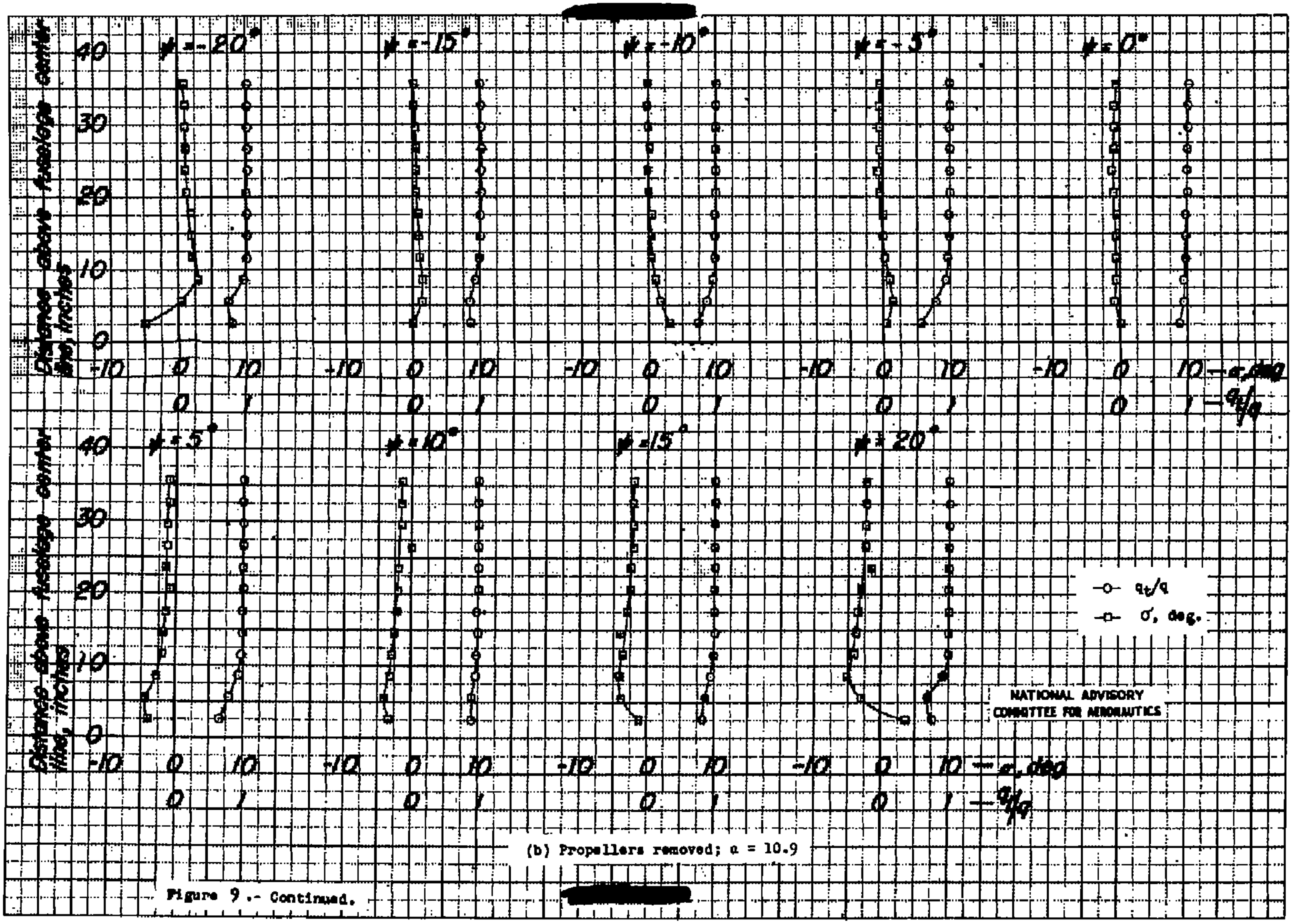

(b) Propellers removed; α = 10.9

Figure 9.- Continued.

[redacted]

2104 9

[redacted]

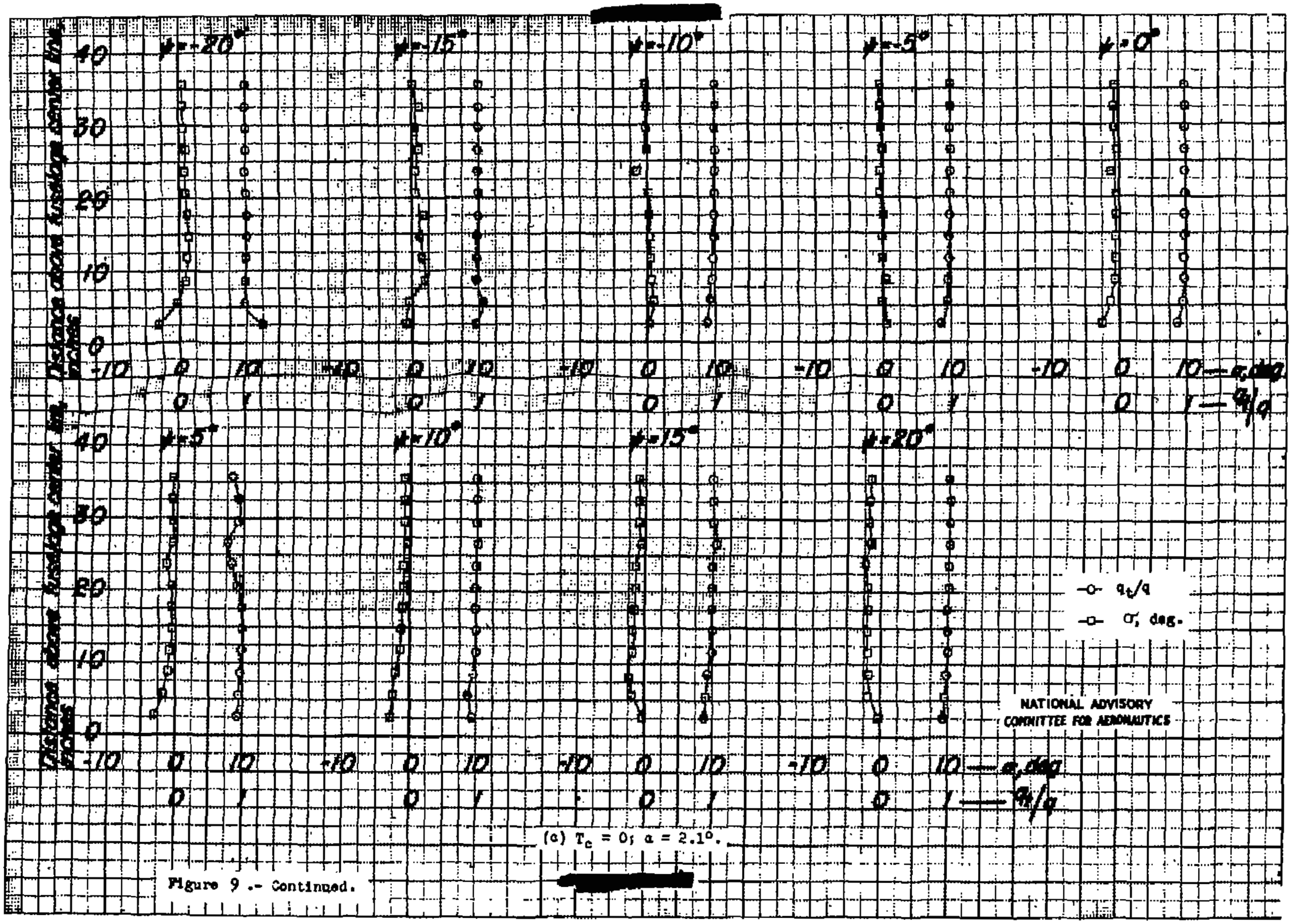

(c) $T_c = 0$; $\alpha = 2.1^{\circ}$.

[redacted]

Figure 9 .- Continued.

[redacted]

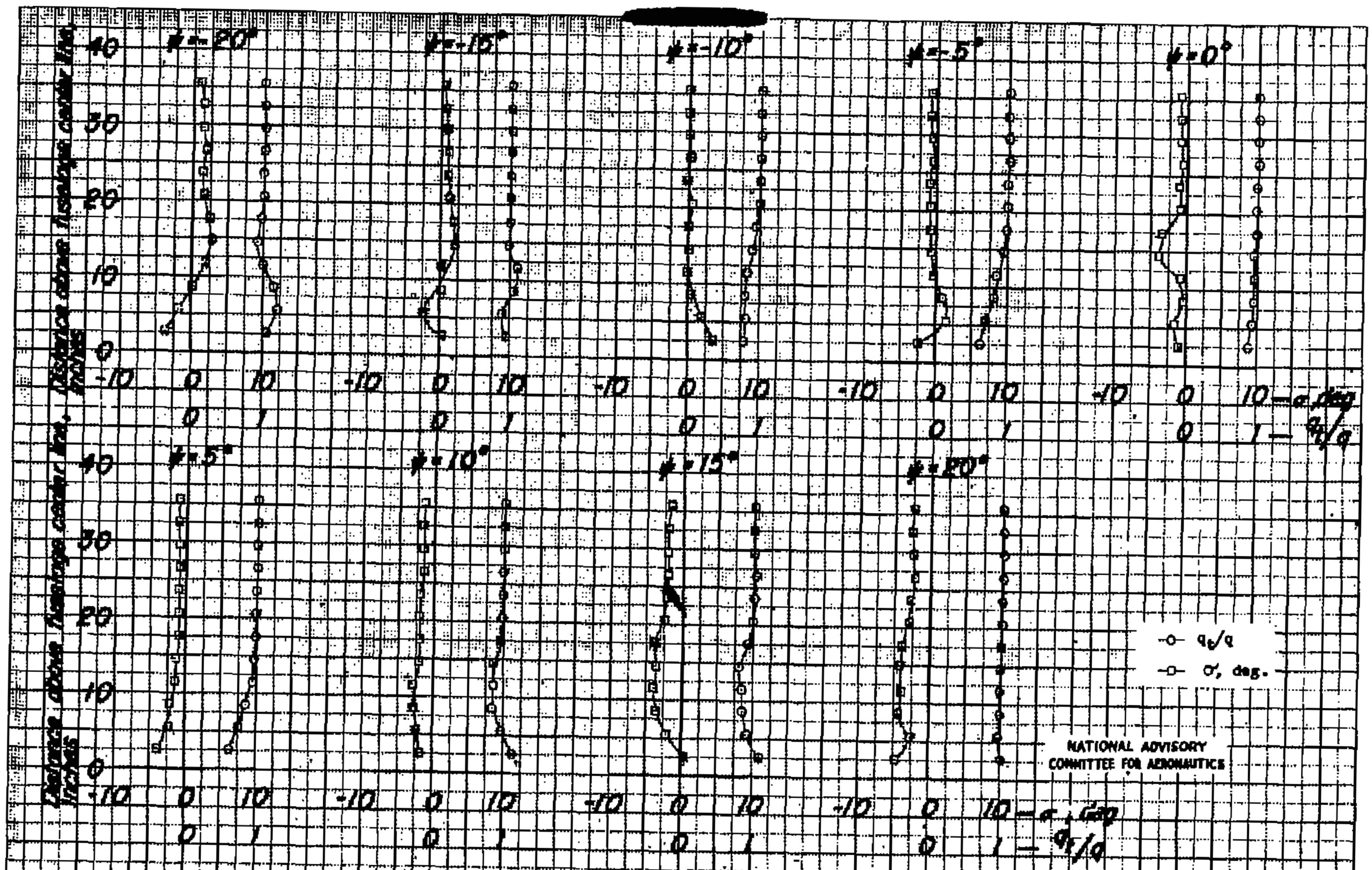

(d) $T_c = 0$; $\alpha = 10.9°$

Figure 9 .- Continued.

[redacted]

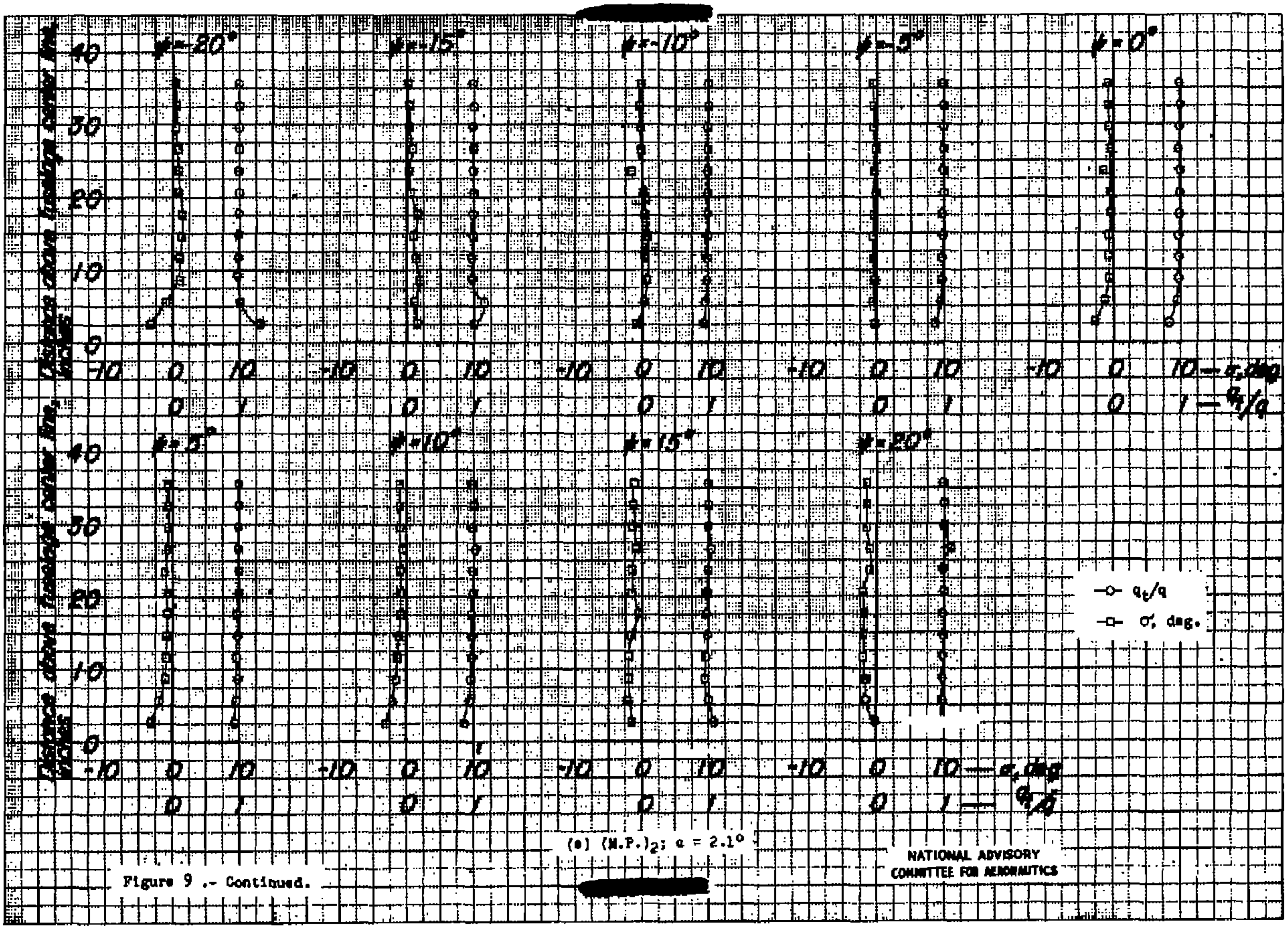

(e) $(M.P.)_2$; $\alpha = 2.1°$

Figure 9 .- Continued.

[redacted]

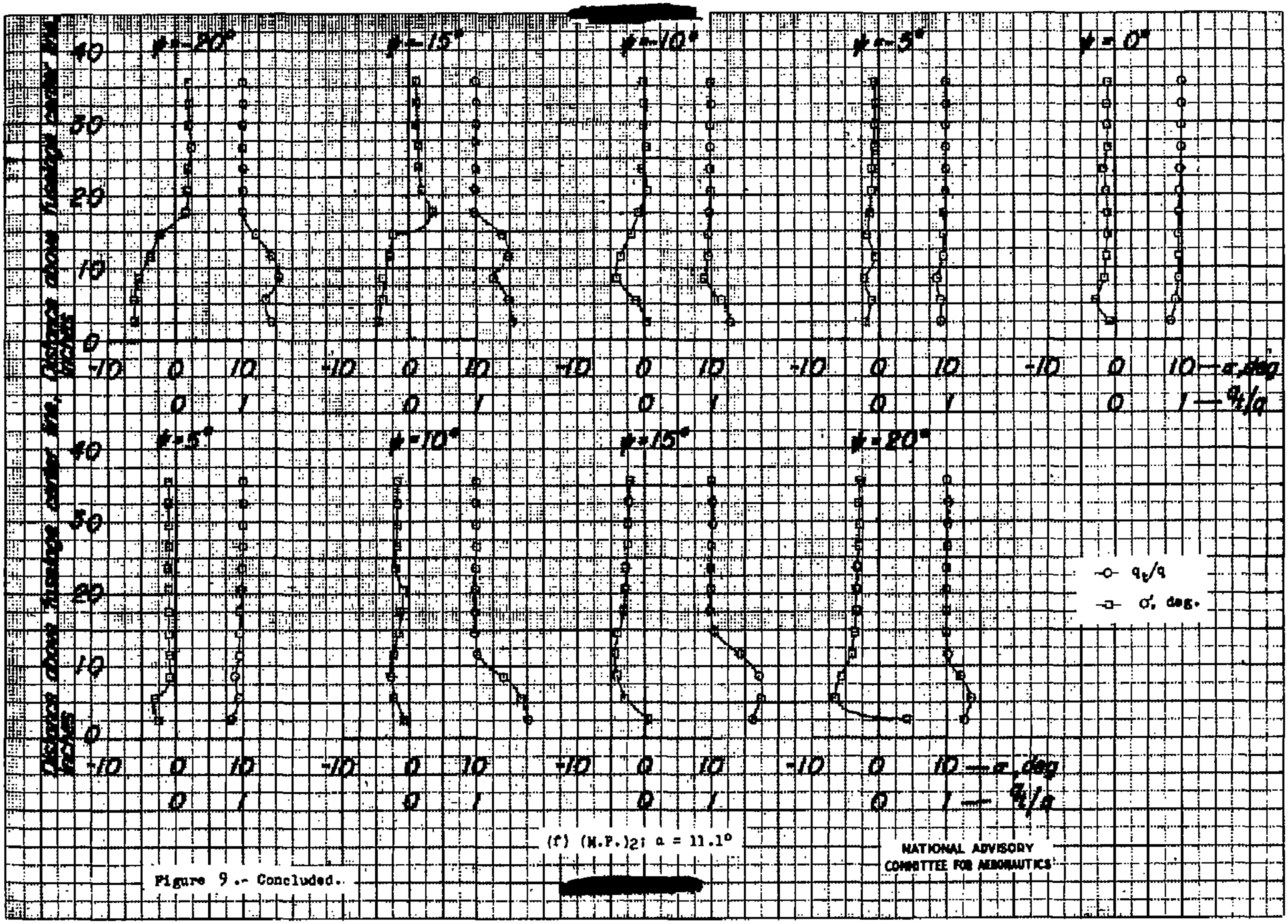

(f) $(M.P.)_2$; $\alpha = 11.1°$

Figure 9.- Concluded.

[redacted]

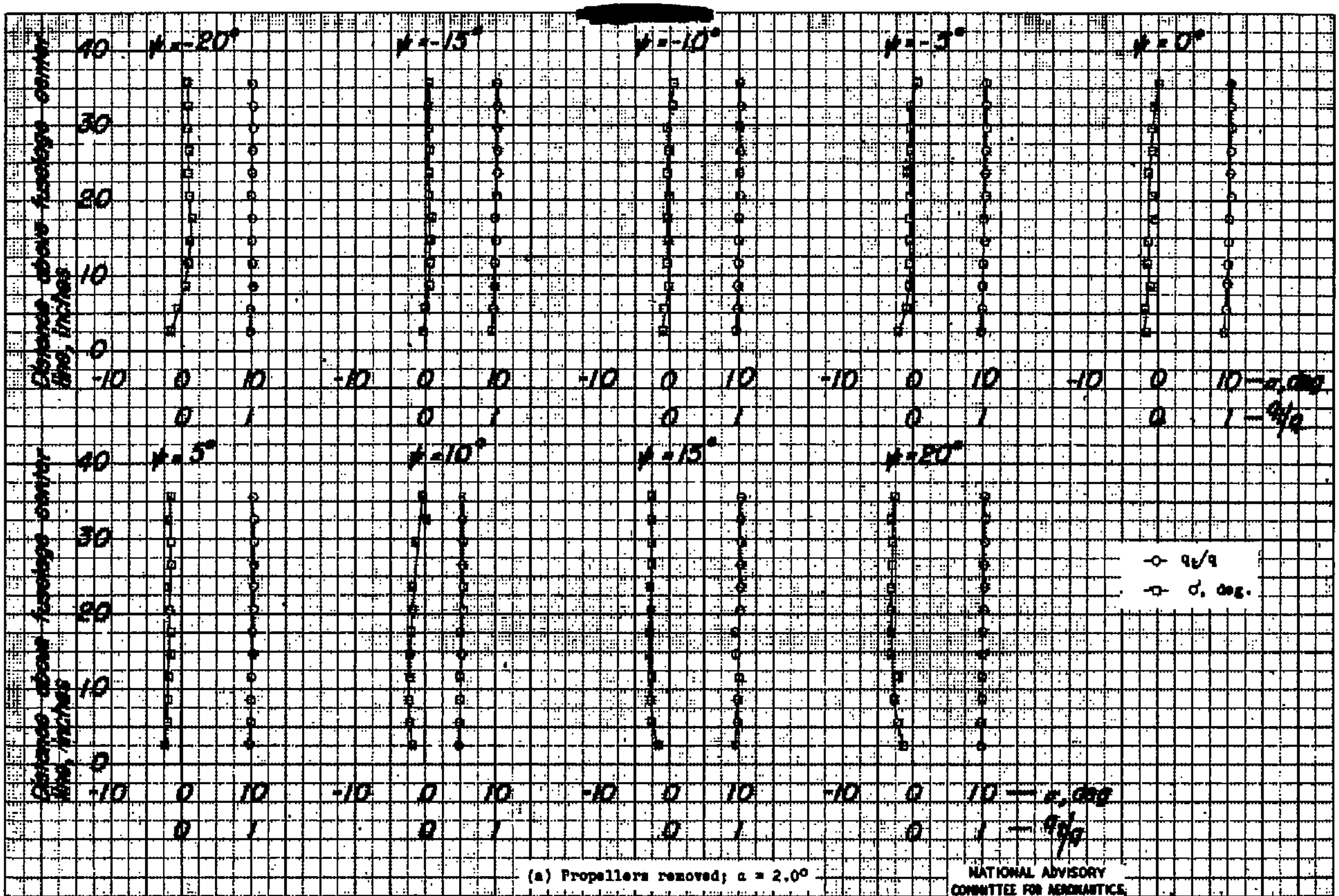

Figure 10.- Variation of sidewash angles and dynamic pressure ratios along the span of the vertical tail for various angles of yaw. $\delta_f = 55^\circ$.

[redacted]

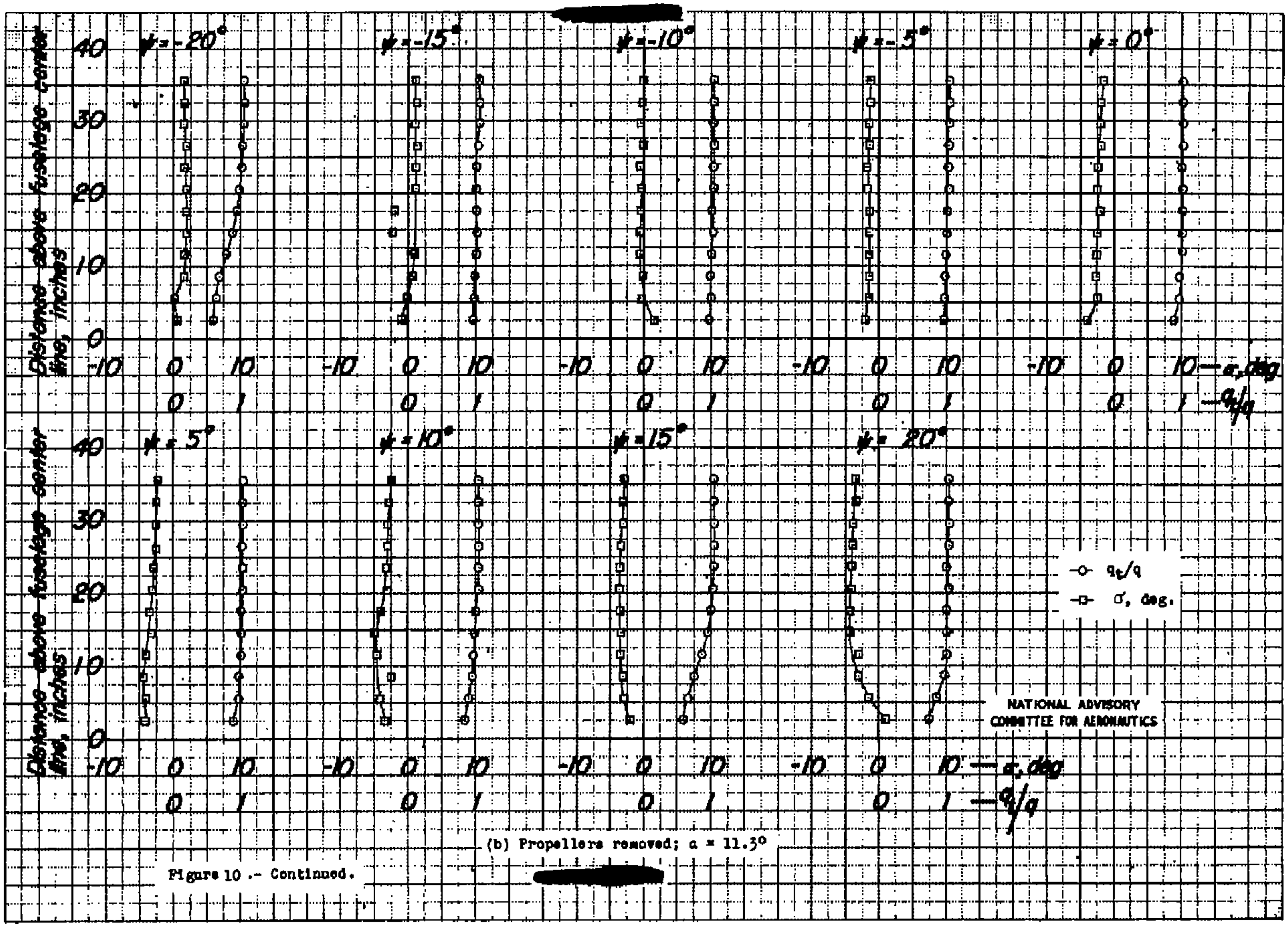

(b) Propellers removed; α = 11.3°

Figure 10 .- Continued.

[redacted]

[redacted]

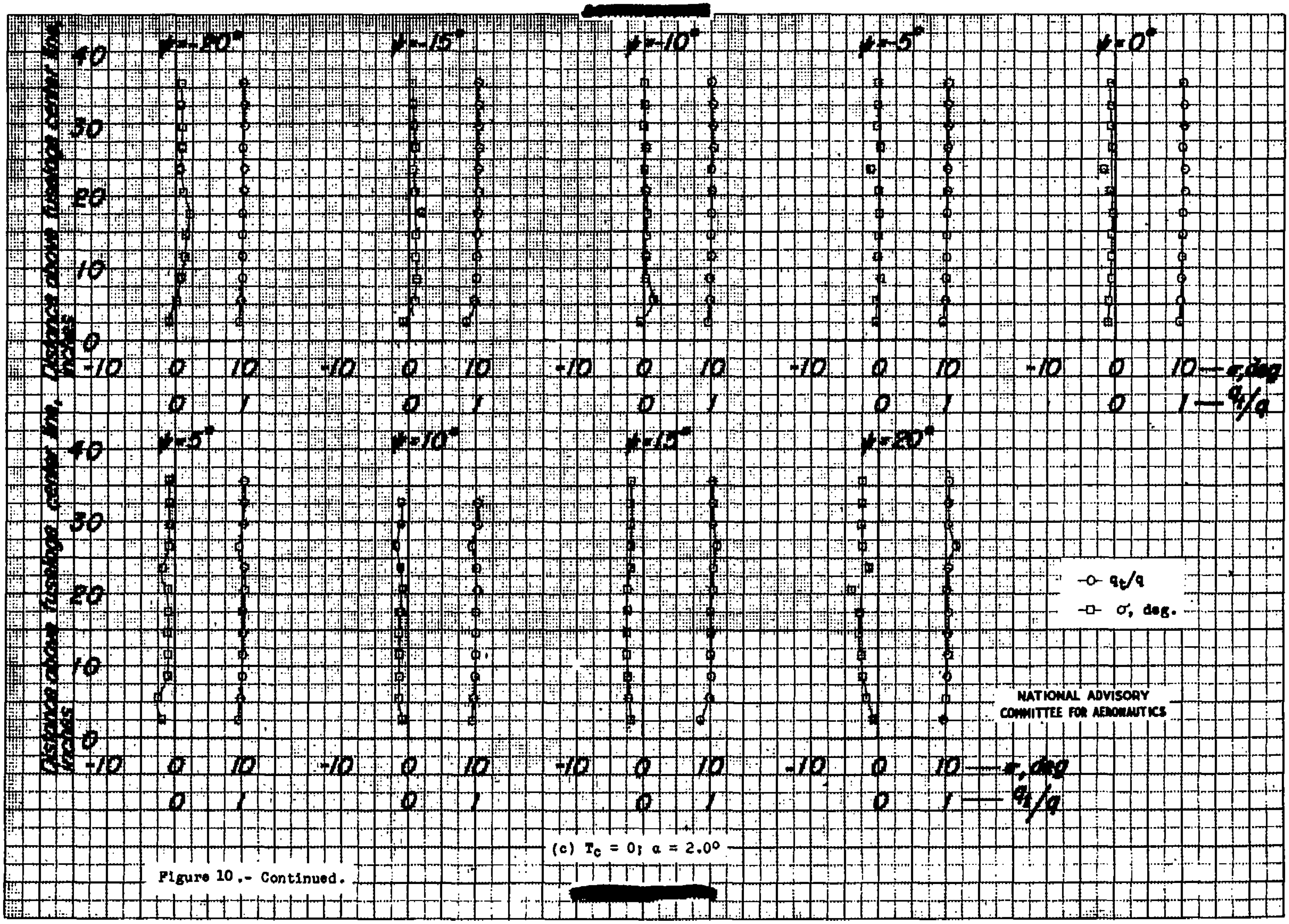

(c) $T_c = 0$; $\alpha = 2.0°$

Figure 10.- Continued.

[redacted]

[redacted]

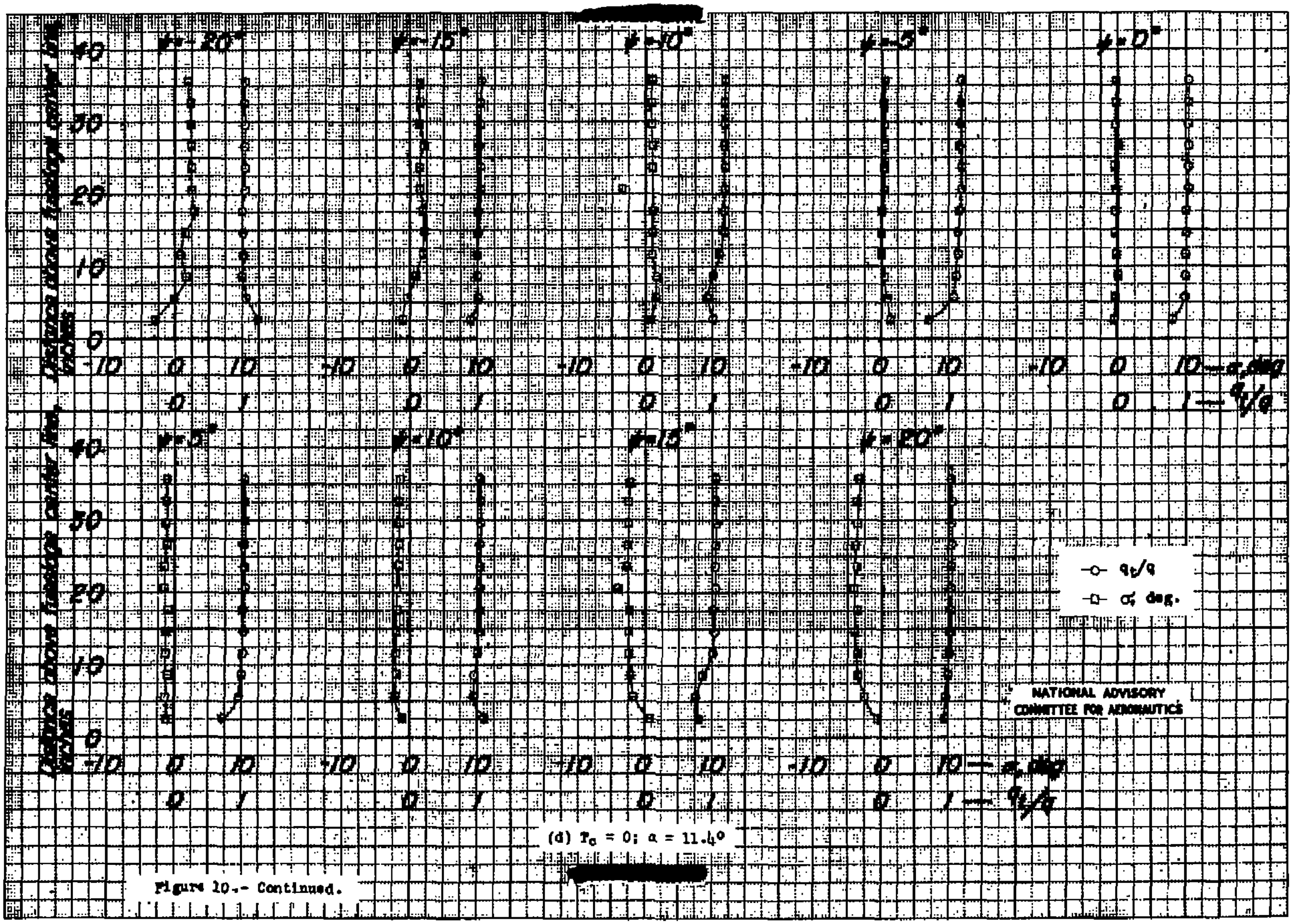

(d) $T_c = 0$; $\alpha = 11.4^{\circ}$

[redacted]

Figure 10.- Continued.

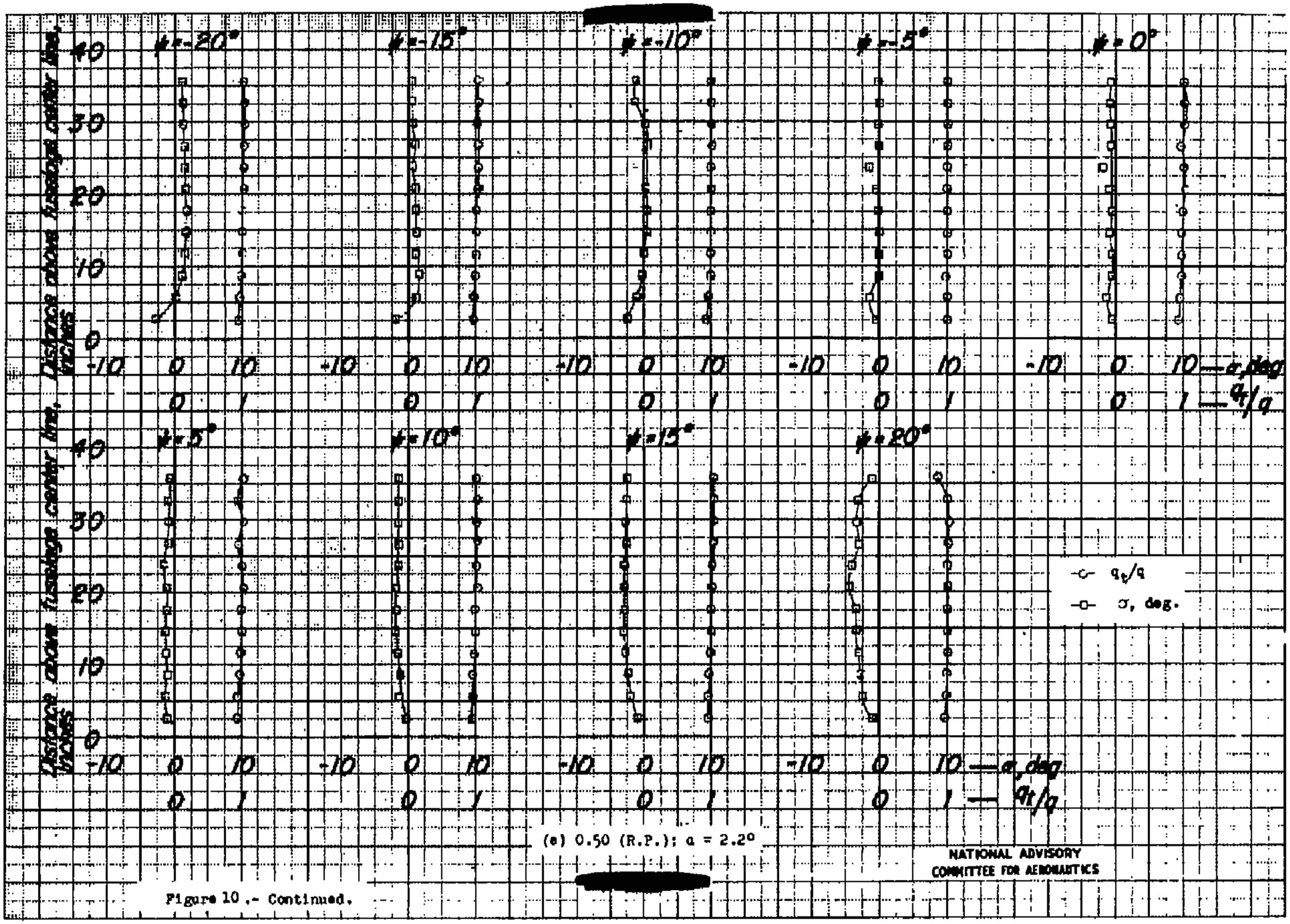

(e) 0.50 (R.P.); α = 2.2°

Figure 10.- Continued.

[redacted]

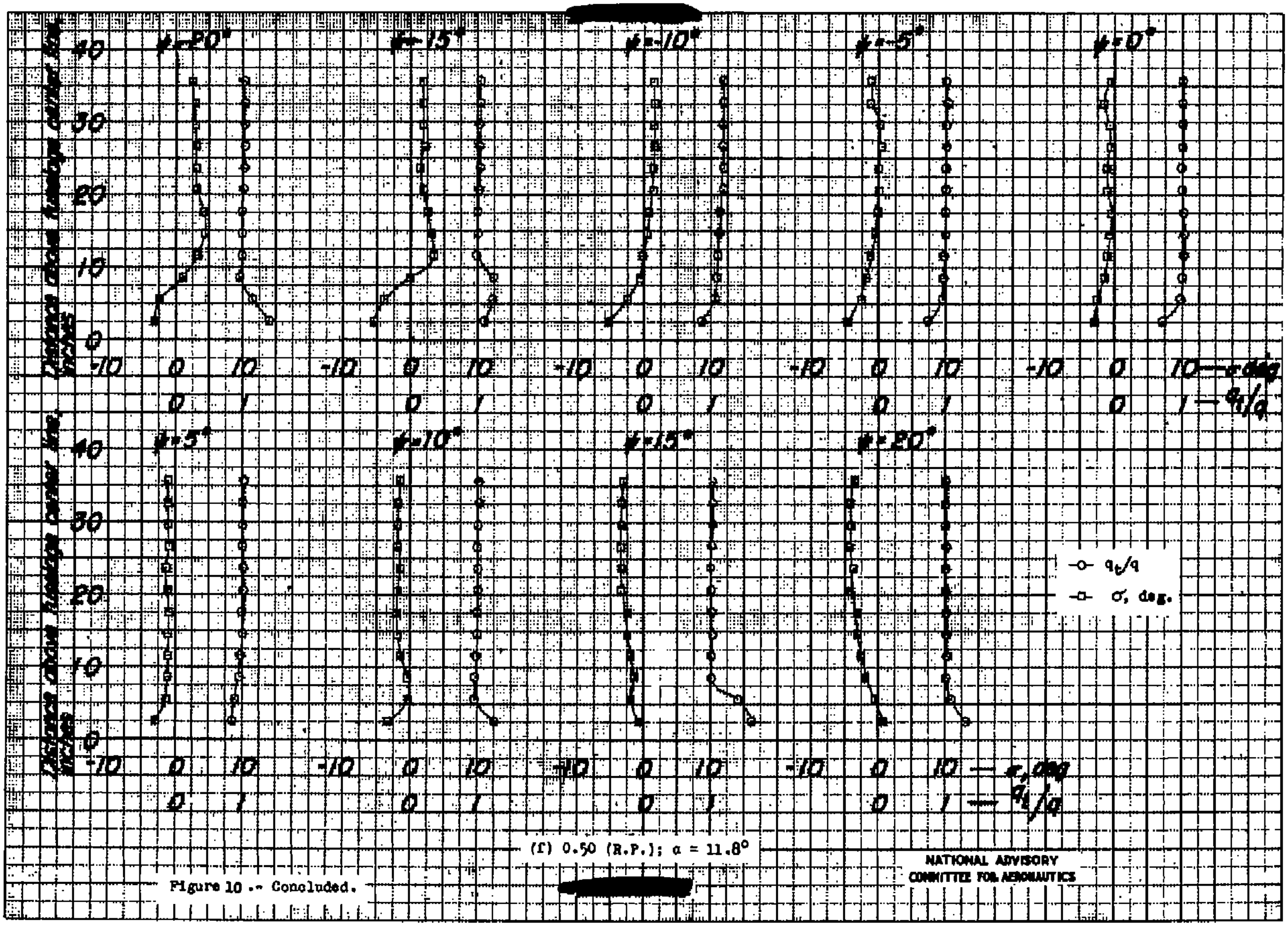

(f) 0.50 (R.P.); α = 11.8°

Figure 10 .- Concluded.

[redacted]

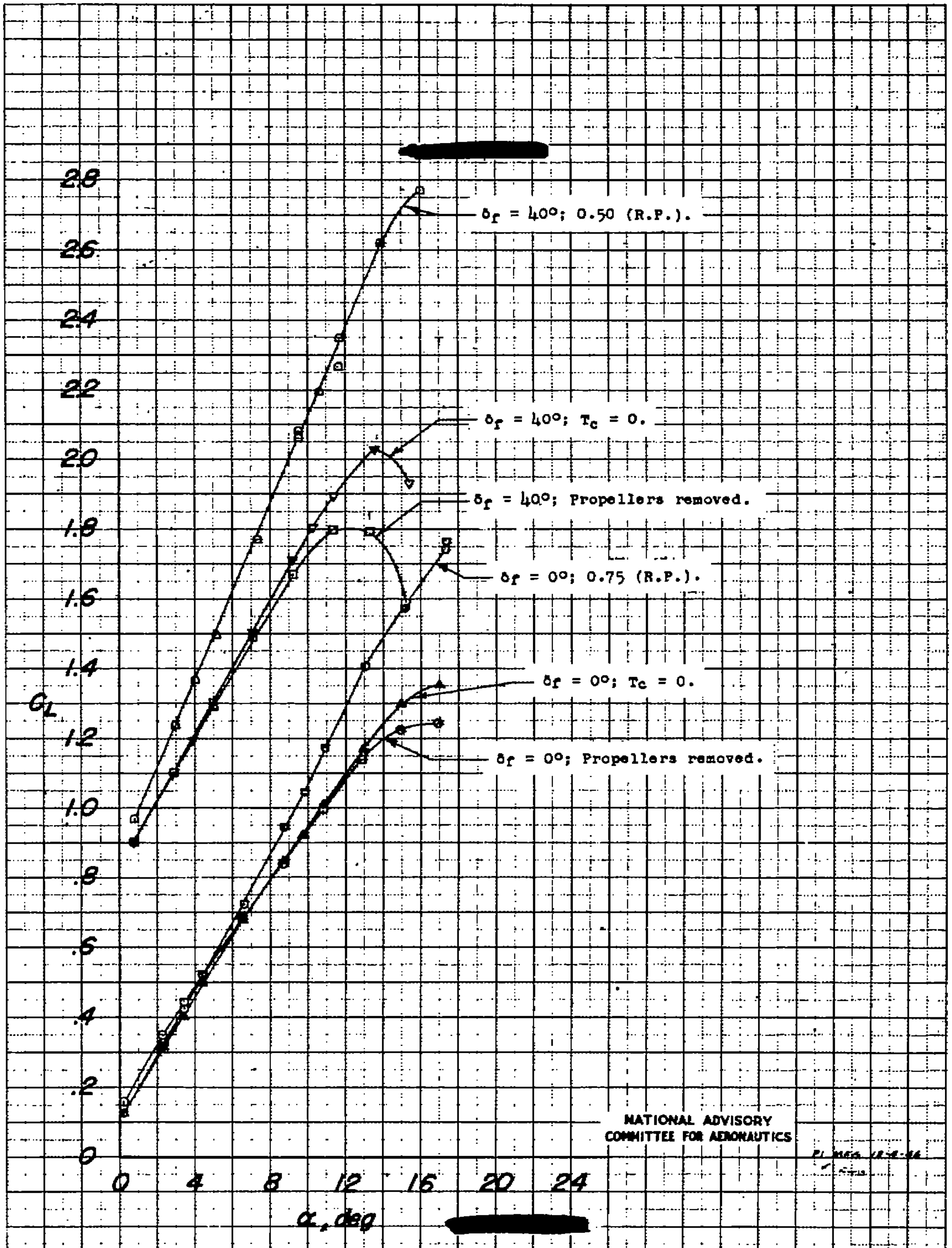

Figure 11.- Tail off lift curves for several flap deflections and power conditions.

[redacted]

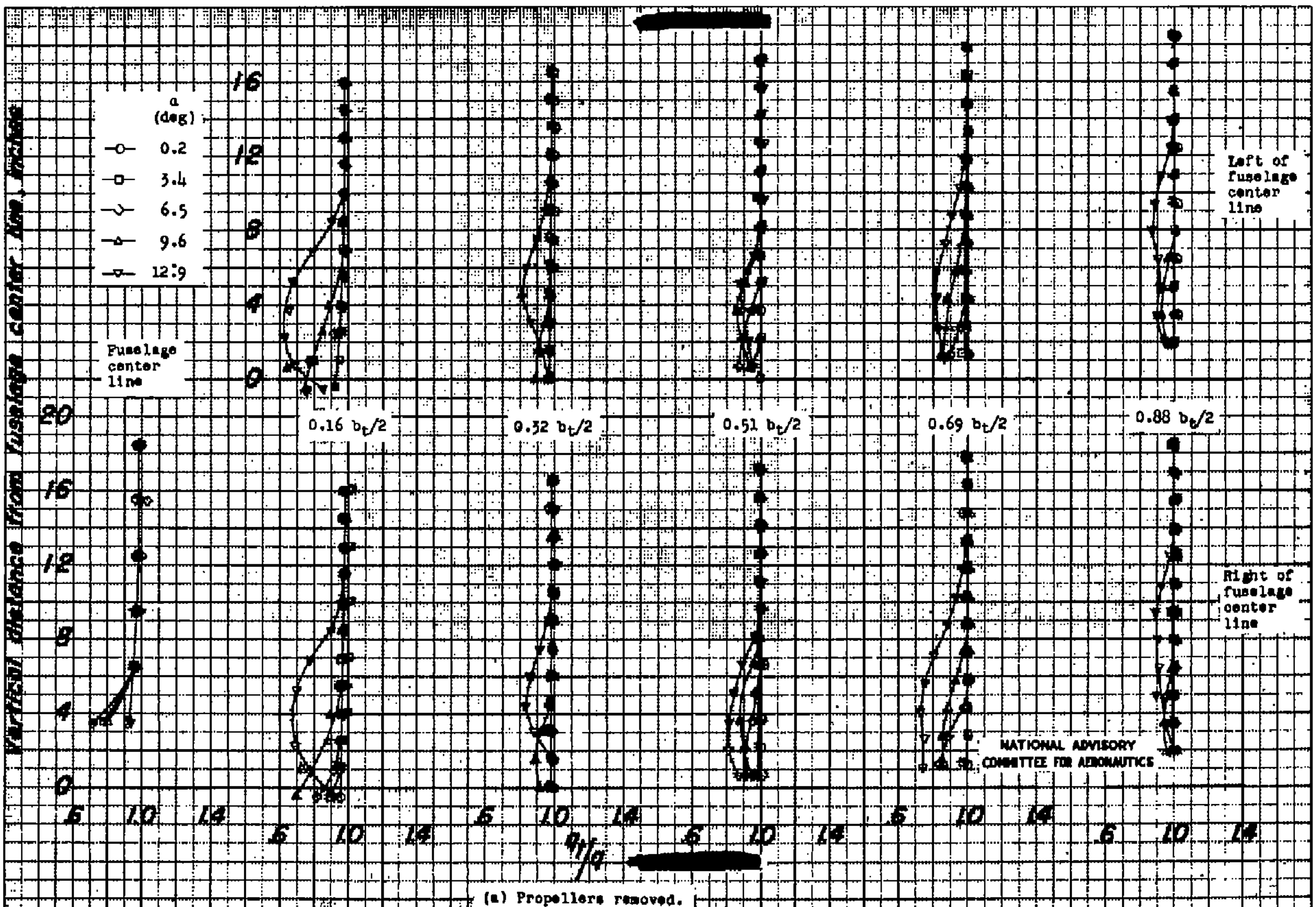

[redacted]

(a) Propellers removed.

Figure 12.- Variation of dynamic pressure ratios in the region of the horizontal tail for several angles of attack. $\delta_f = 0^\circ$.

[redacted]

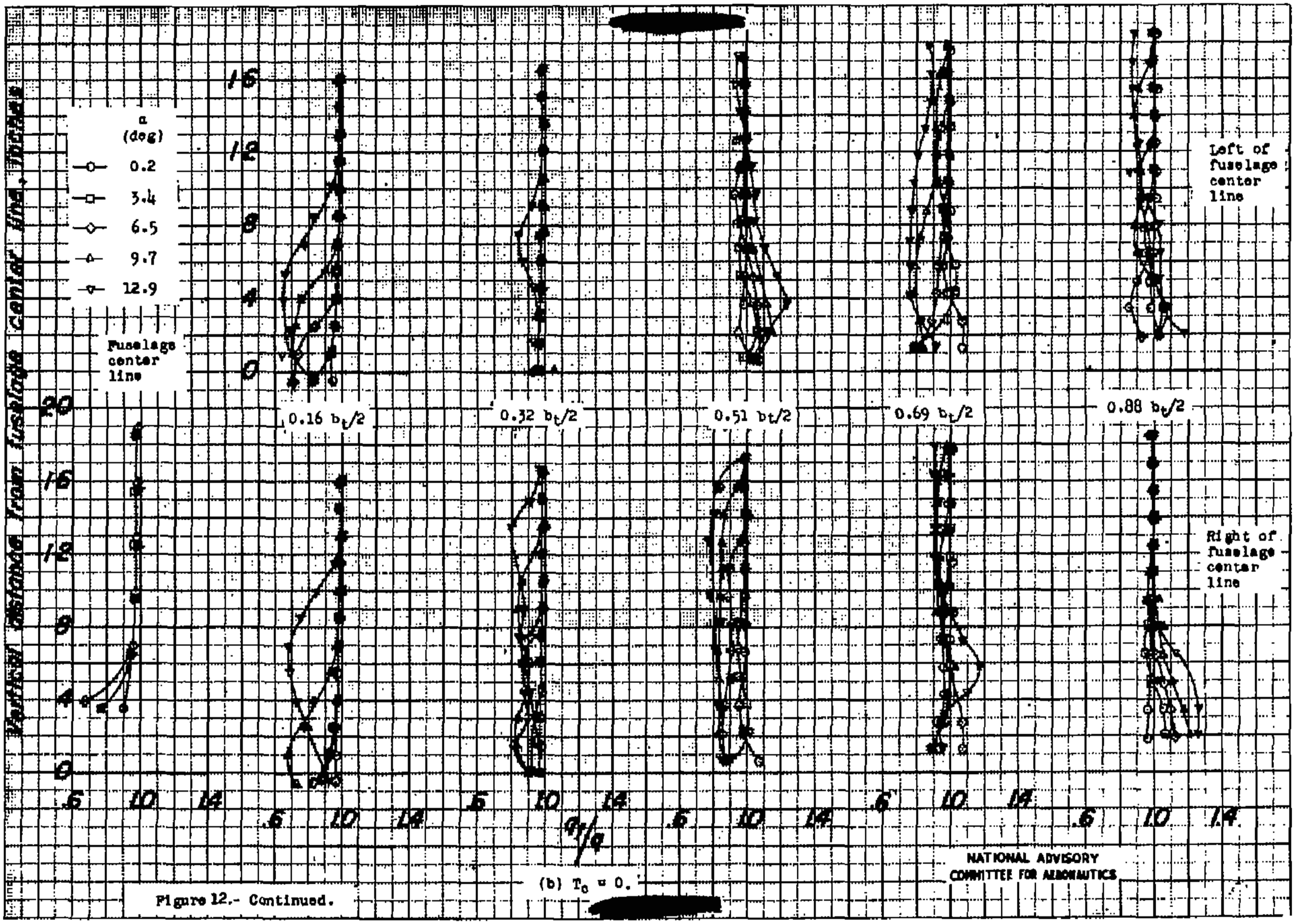

(b) $T_c = 0$.

Figure 12.- Continued.

[redacted]

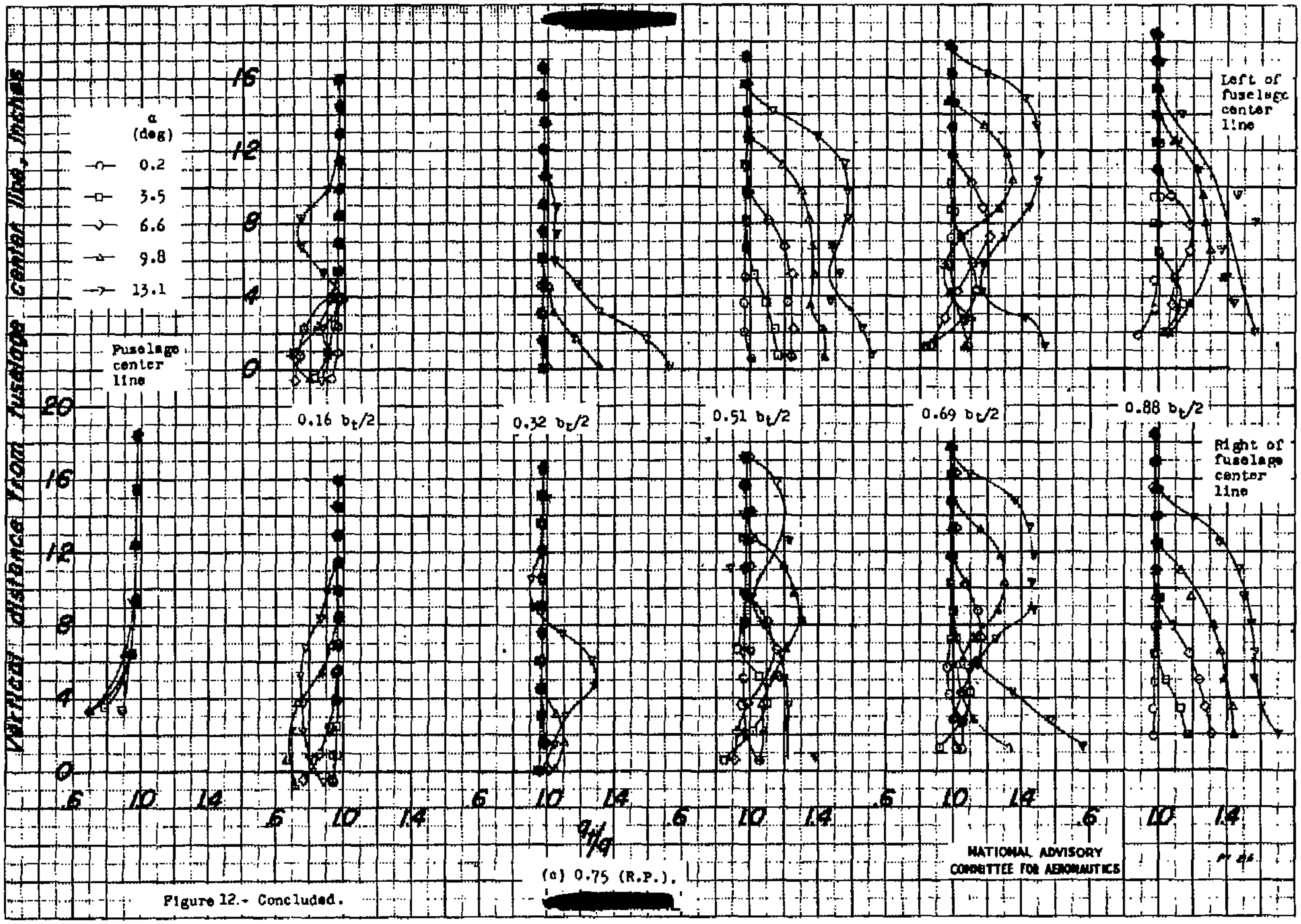

(c) 0.75 (R.P.).

Figure 12.- Concluded.

21041

[redacted]

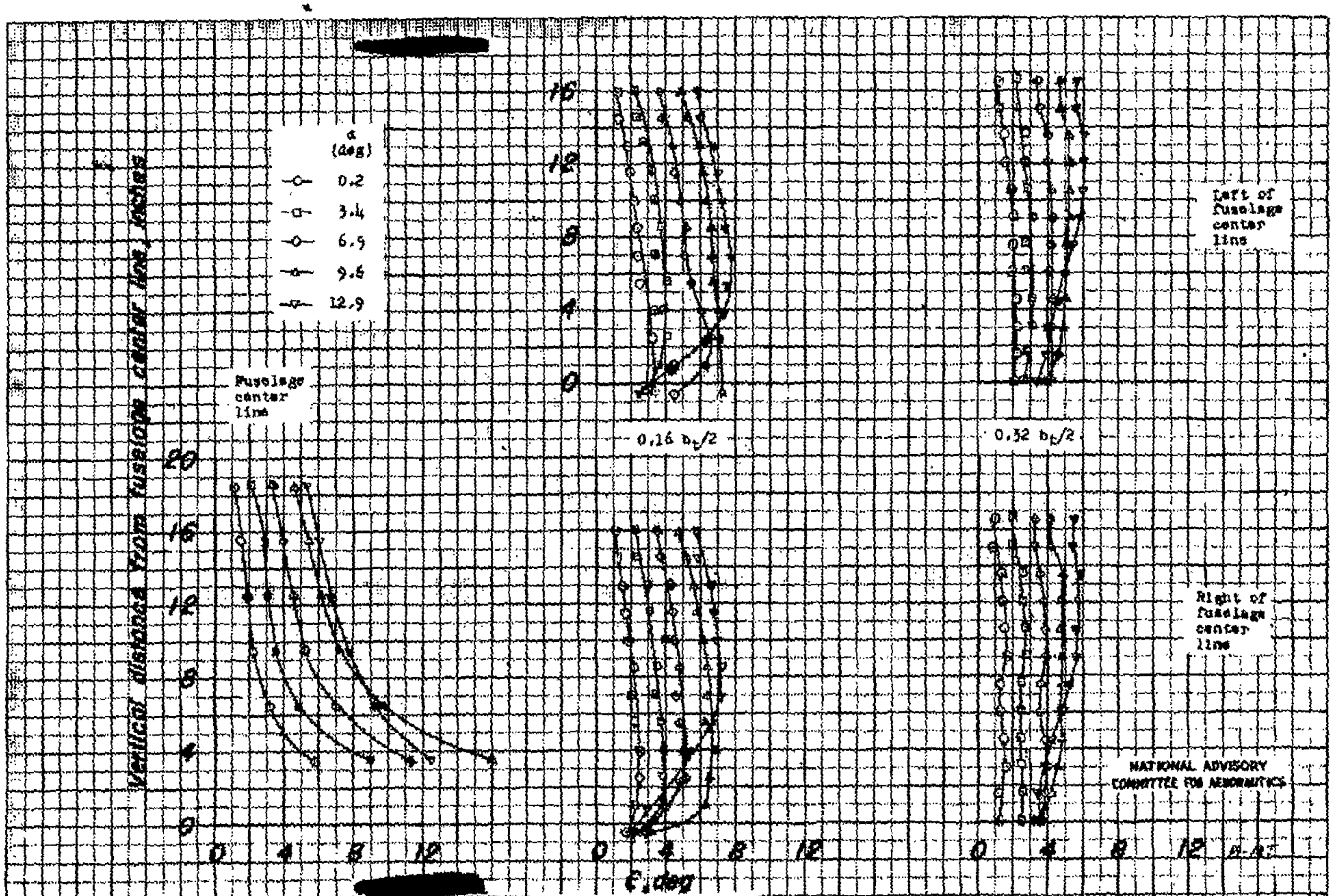

[redacted]

(a) Propellers removed.

Figure 13.- Variation of downwash angles in the region of the horizontal tail for several angles of attack. $\delta_t = 0°$.

[redacted]

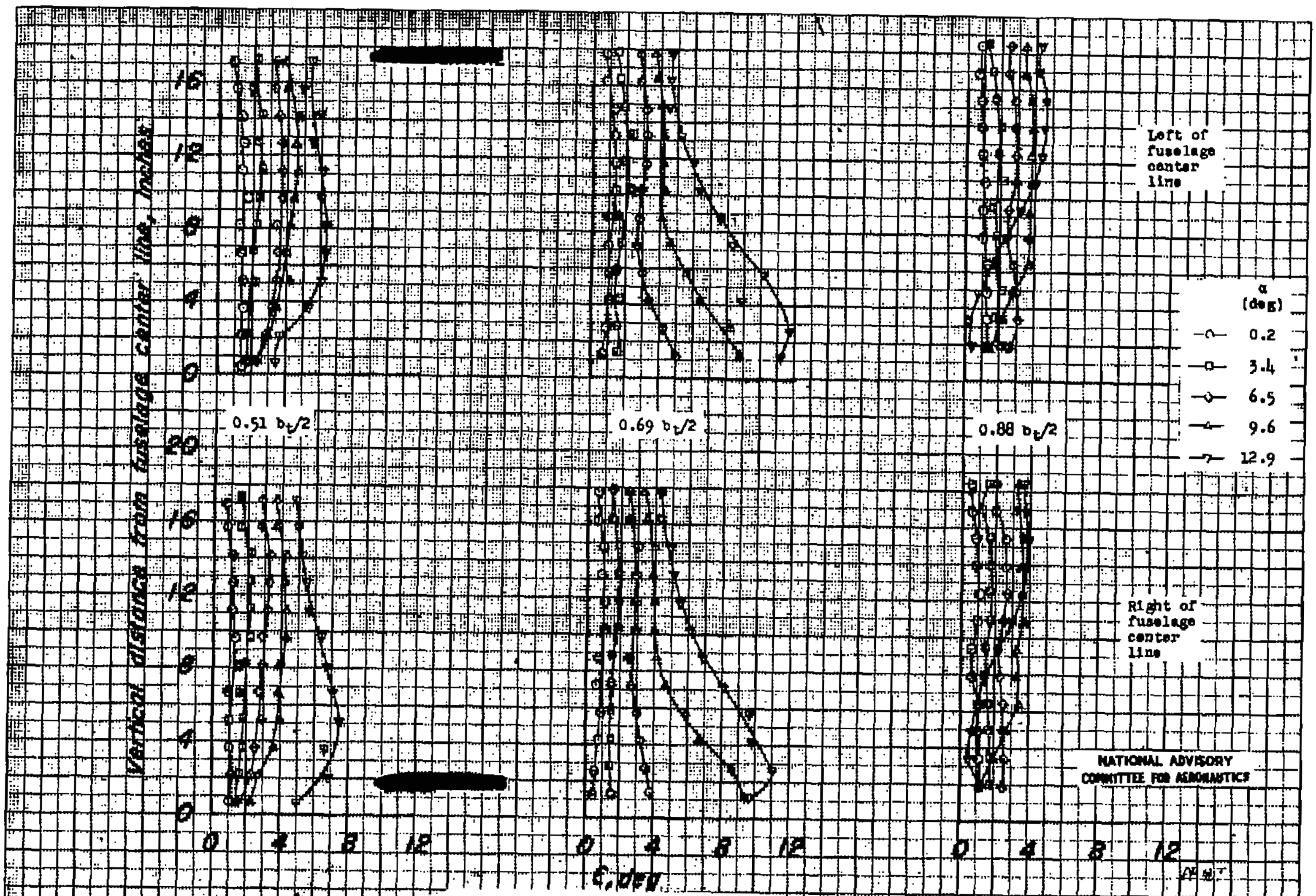

[redacted]

Figure 13 .- Continued. (a) Concluded; propellers removed.

210413

[redacted]

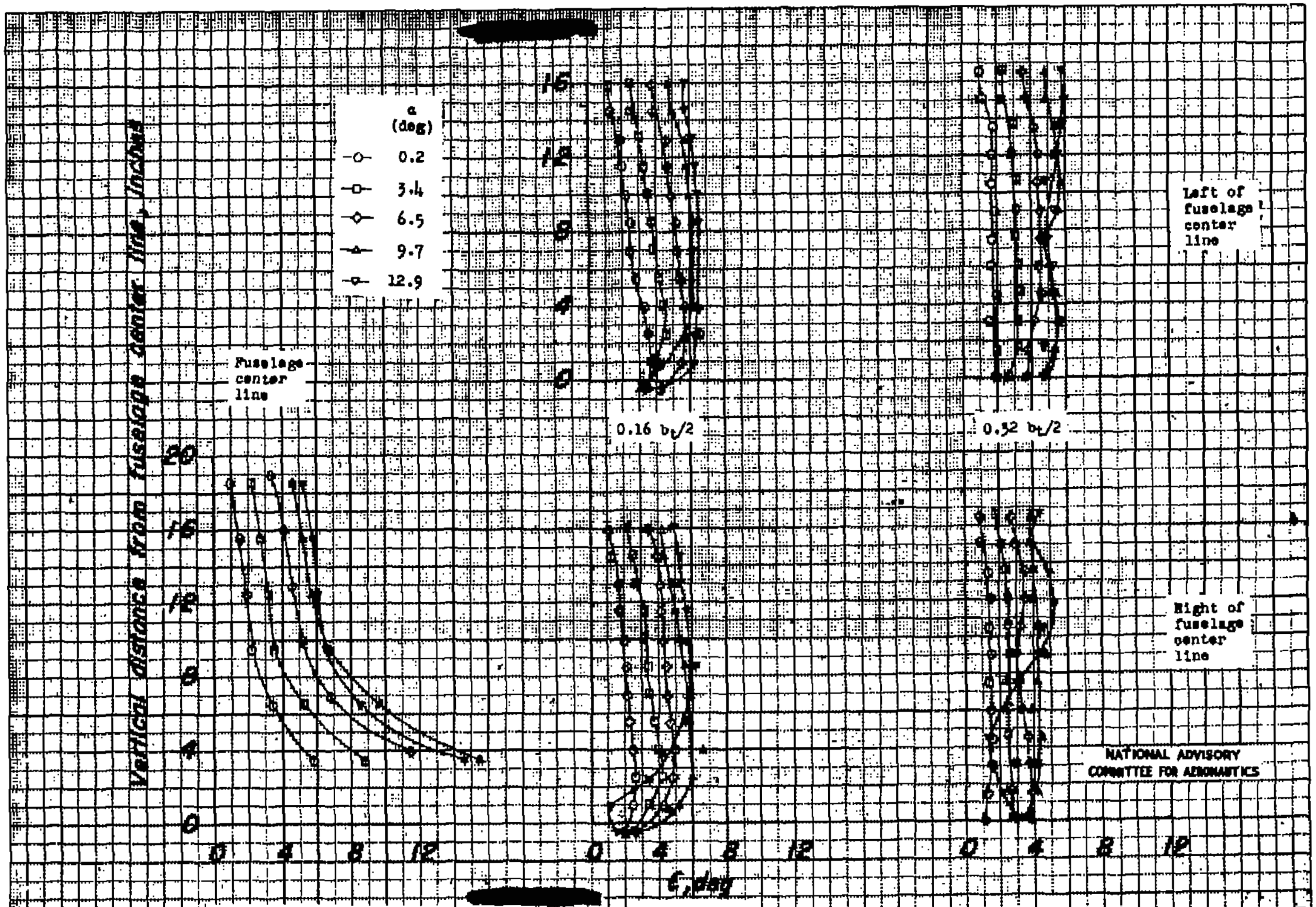

[redacted]

Figure 13.- Continued. (b) $T_c = 0$.

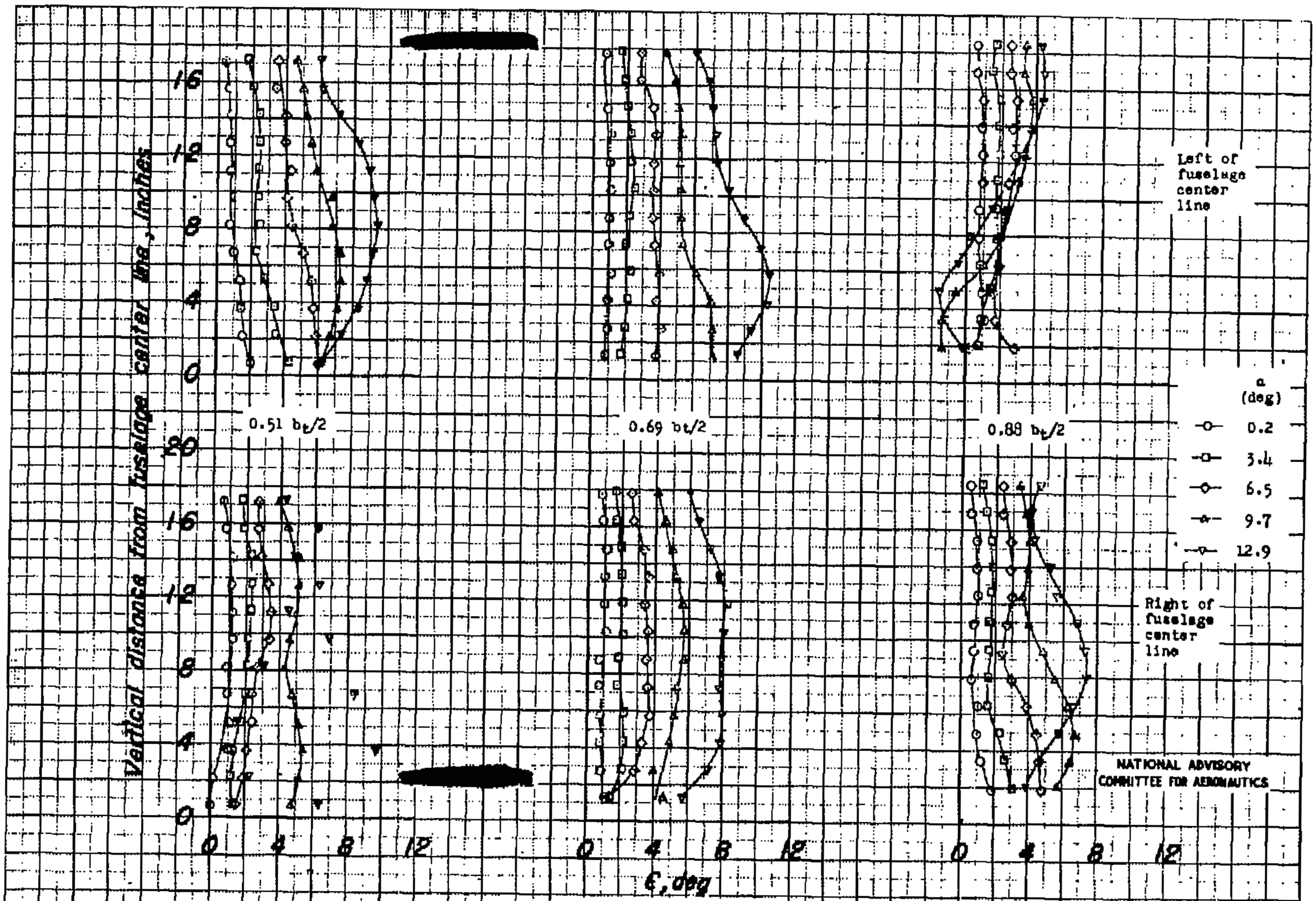

Figure 13.- Continued. (b) Concluded; $T_c = 0$.

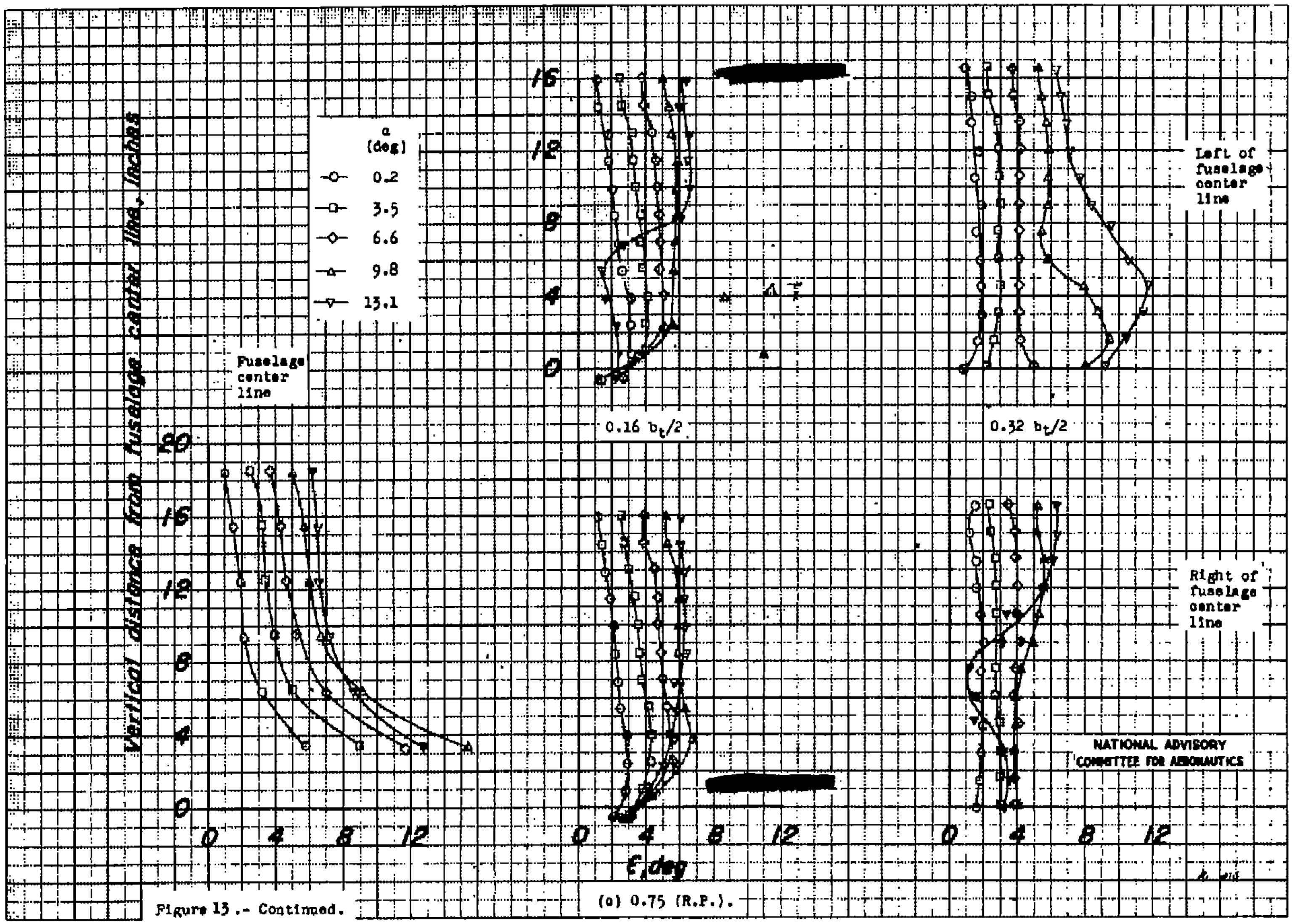

Figure 13 .- Continued.

[redacted]

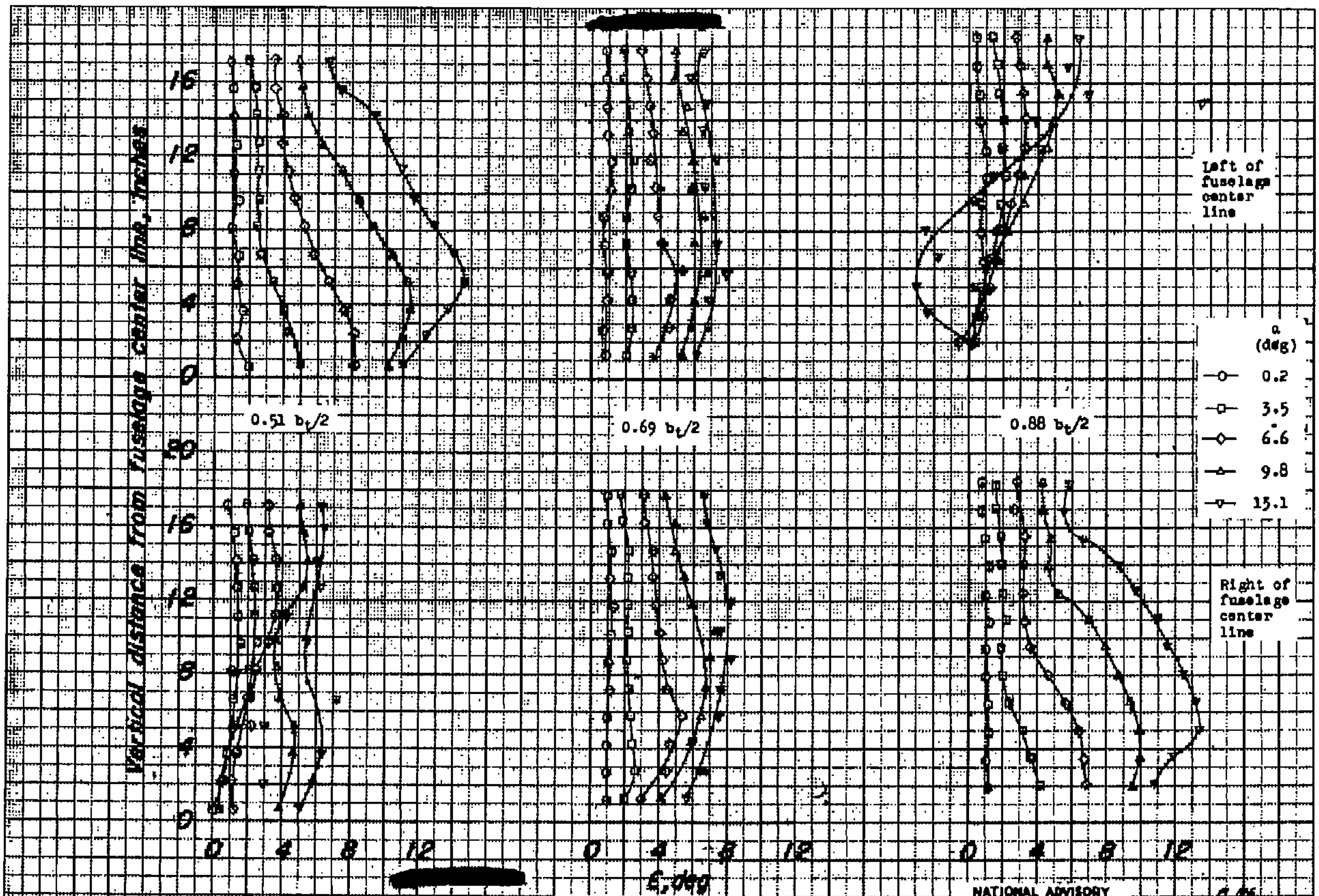

[redacted]

Figure 13.- Concluded. (c) Concluded; 0.75 (R.P.).

[redacted]

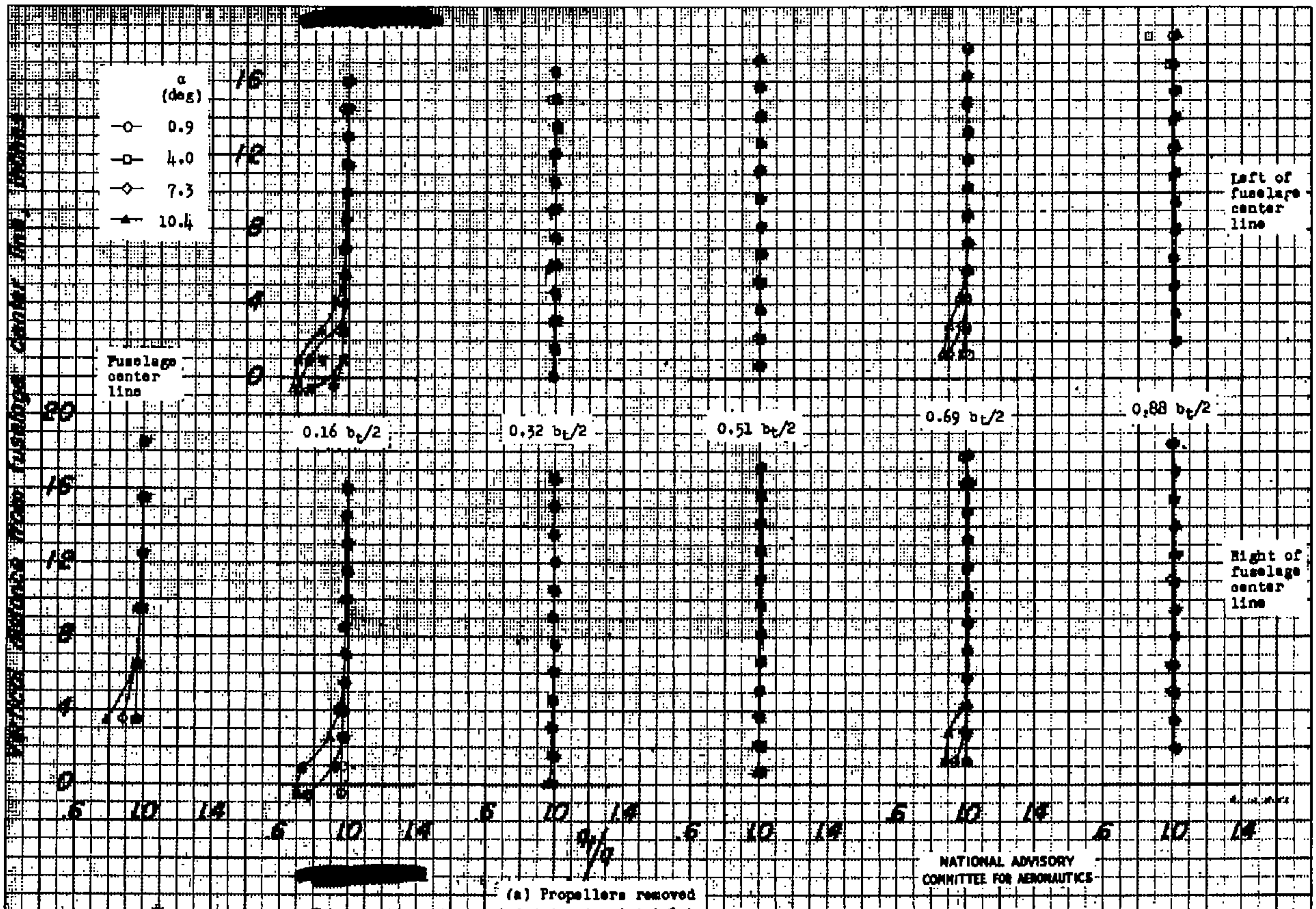

[redacted]

(a) Propellers removed

Figure 14.- Variation of dynamic pressure ratios in the region of the horizontal tail for several angles of attack. $\delta_f = 40^\circ$.

210414

[redacted]

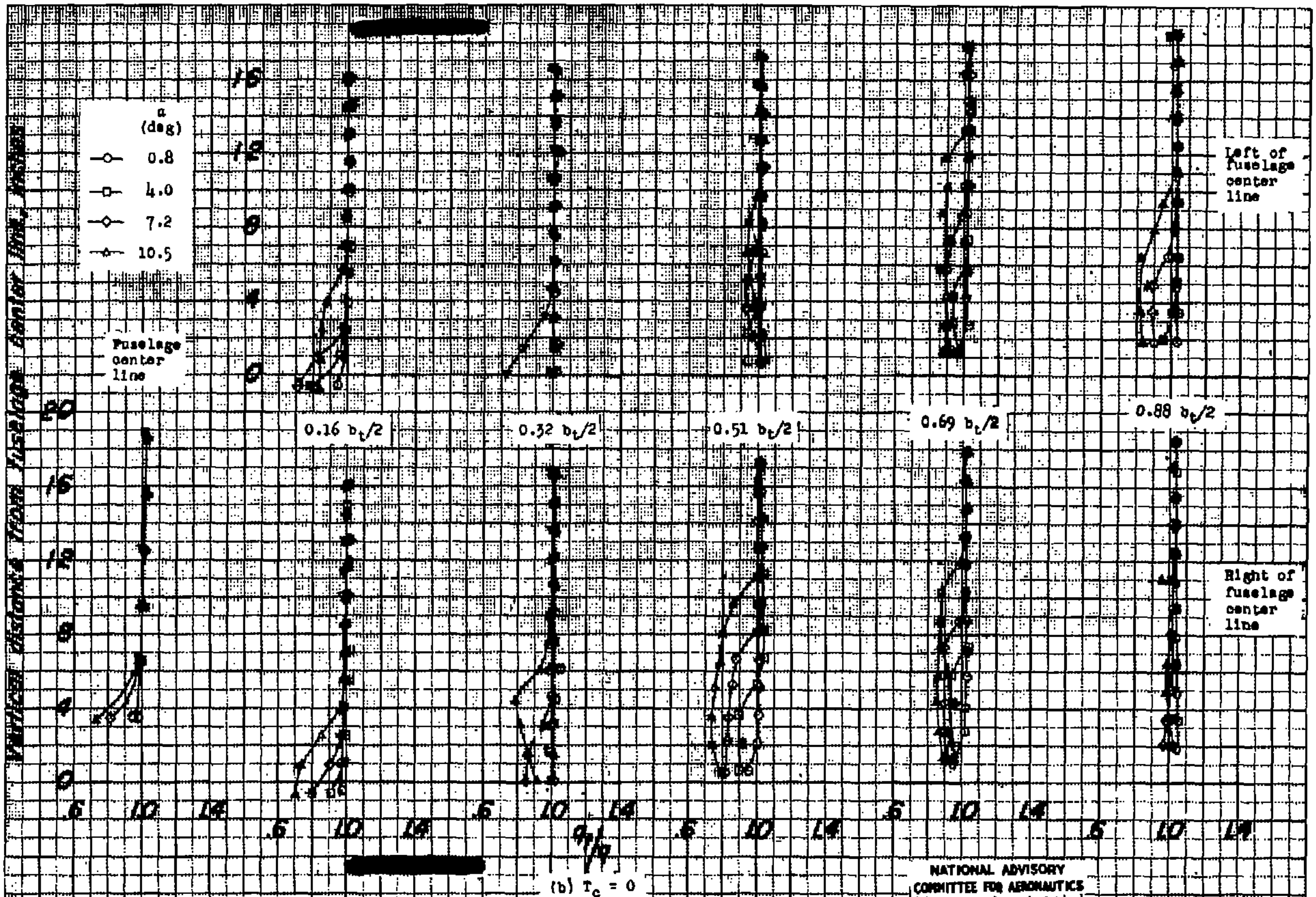

[redacted]

Figure 14 .- Continued.

21041 4

[redacted]

[redacted]

NATIONAL ADVISORY COMMITTEE FOR AERONAUTICS

(c) 0.80(R.P.)

Figure 14.- Concluded.

(a) Propellers removed.

Figure 15.- Variation of downwash angles in the region of the horizontal tail for several angles of attack. $\delta_f = 40^{\circ}$.

210415

NACA RM No. L7D09

[redacted]

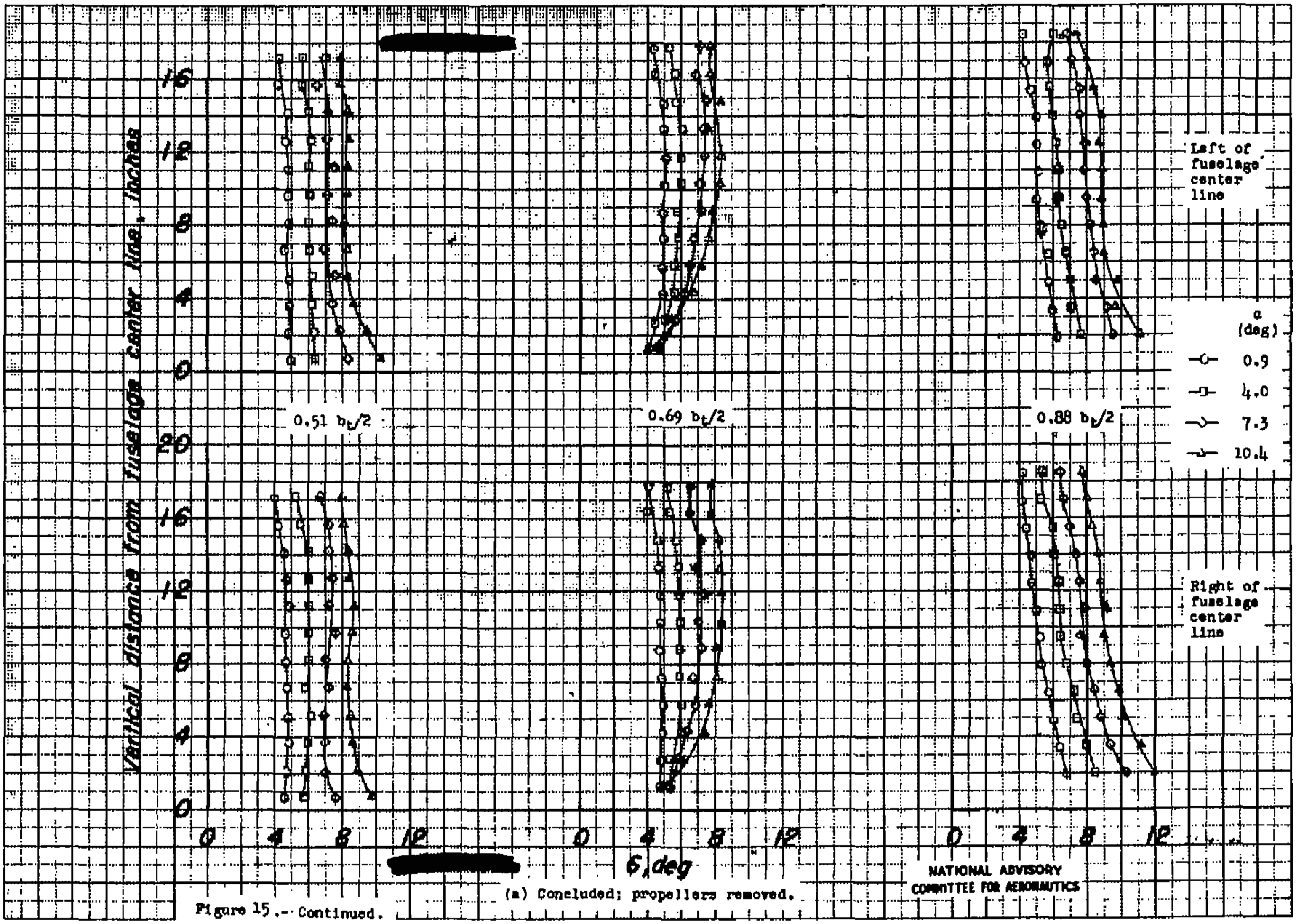

[redacted]

(a) Concluded; propellers removed.

Figure 15.- Continued.

Fig. 15a conc.

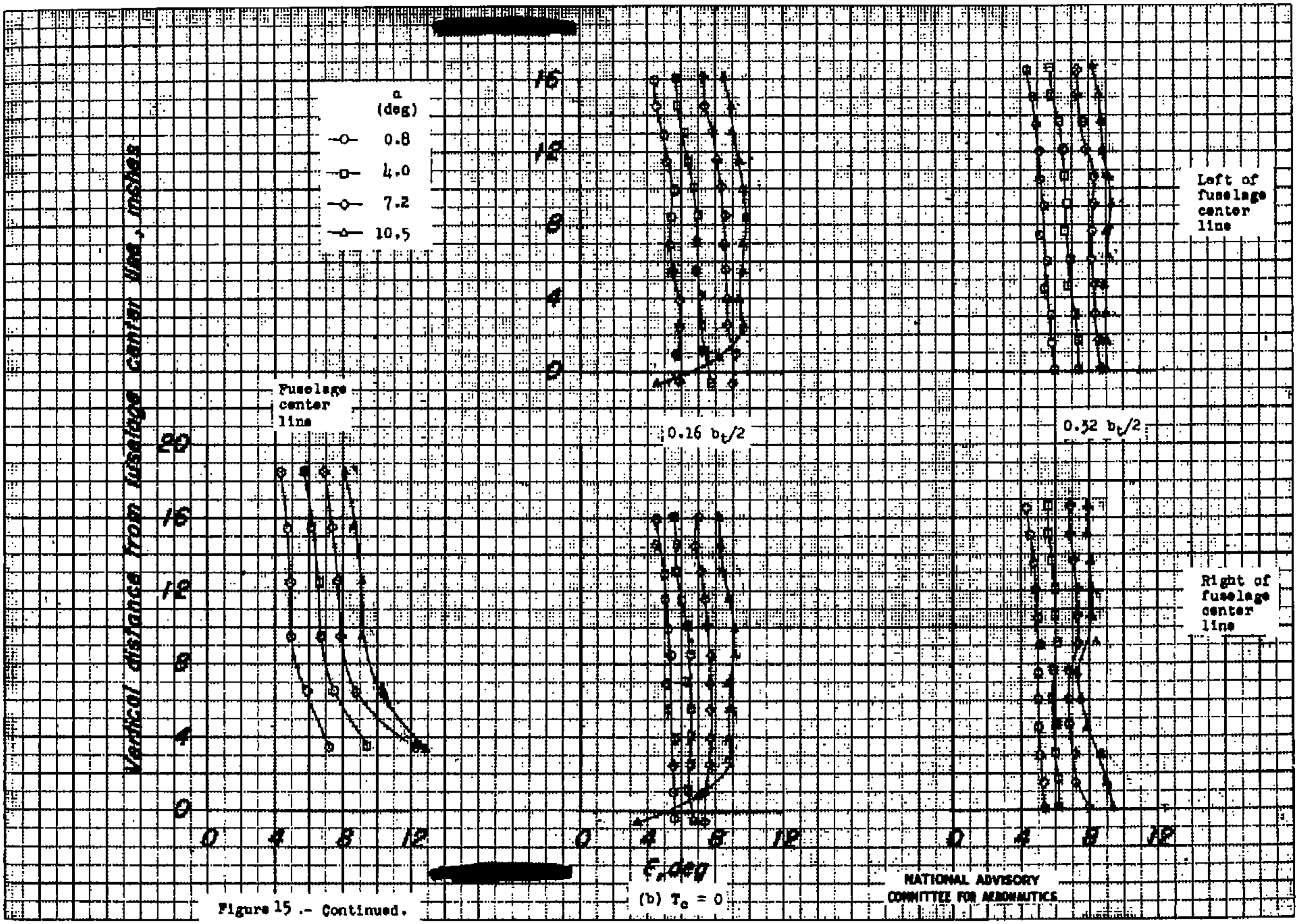

(b) $T_c = 0$

Figure 15 .- Continued.

[redacted]

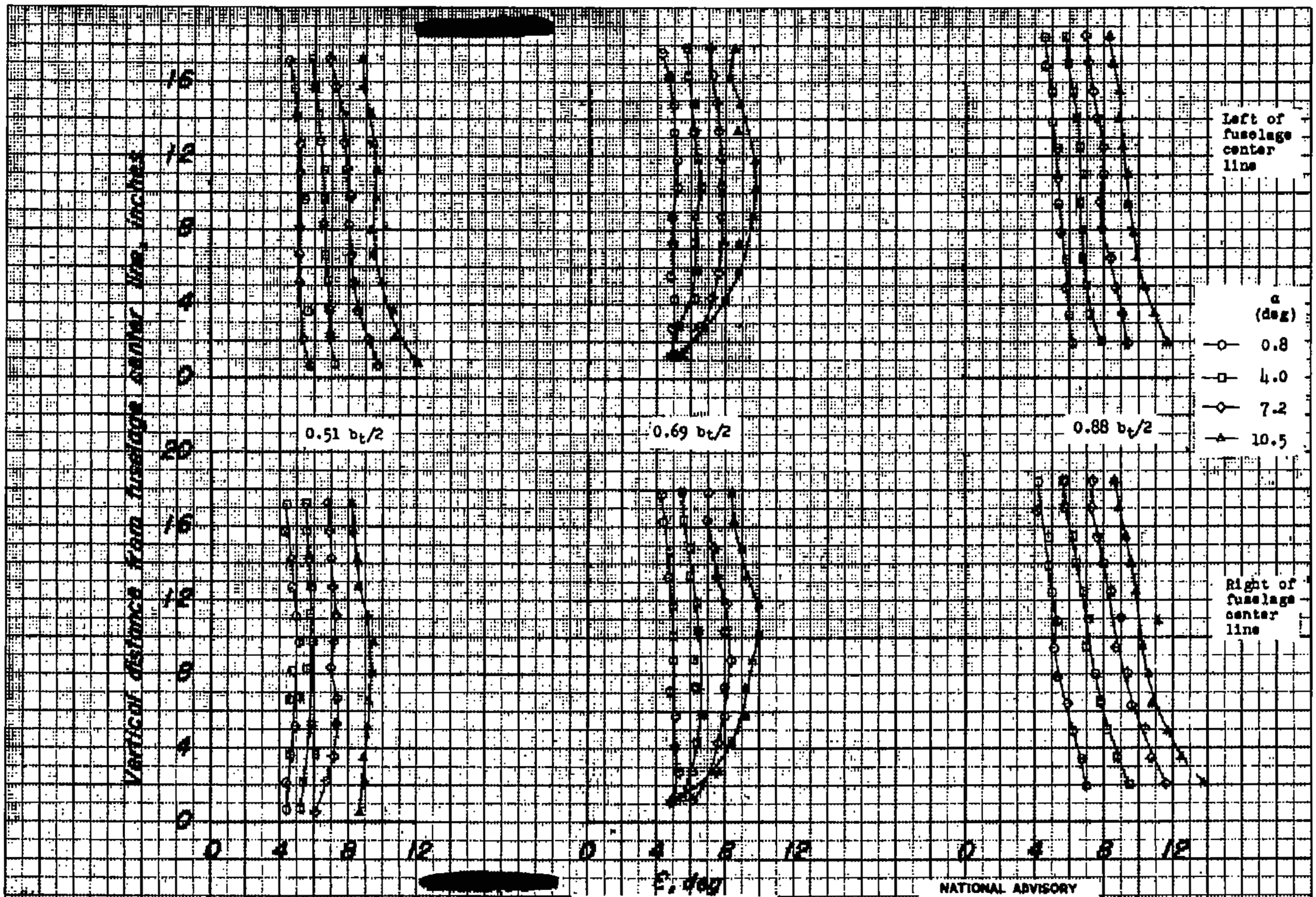

[redacted]

Figure 15.- Continued.

(b) Concluded: $T_c = 0$

[redacted]

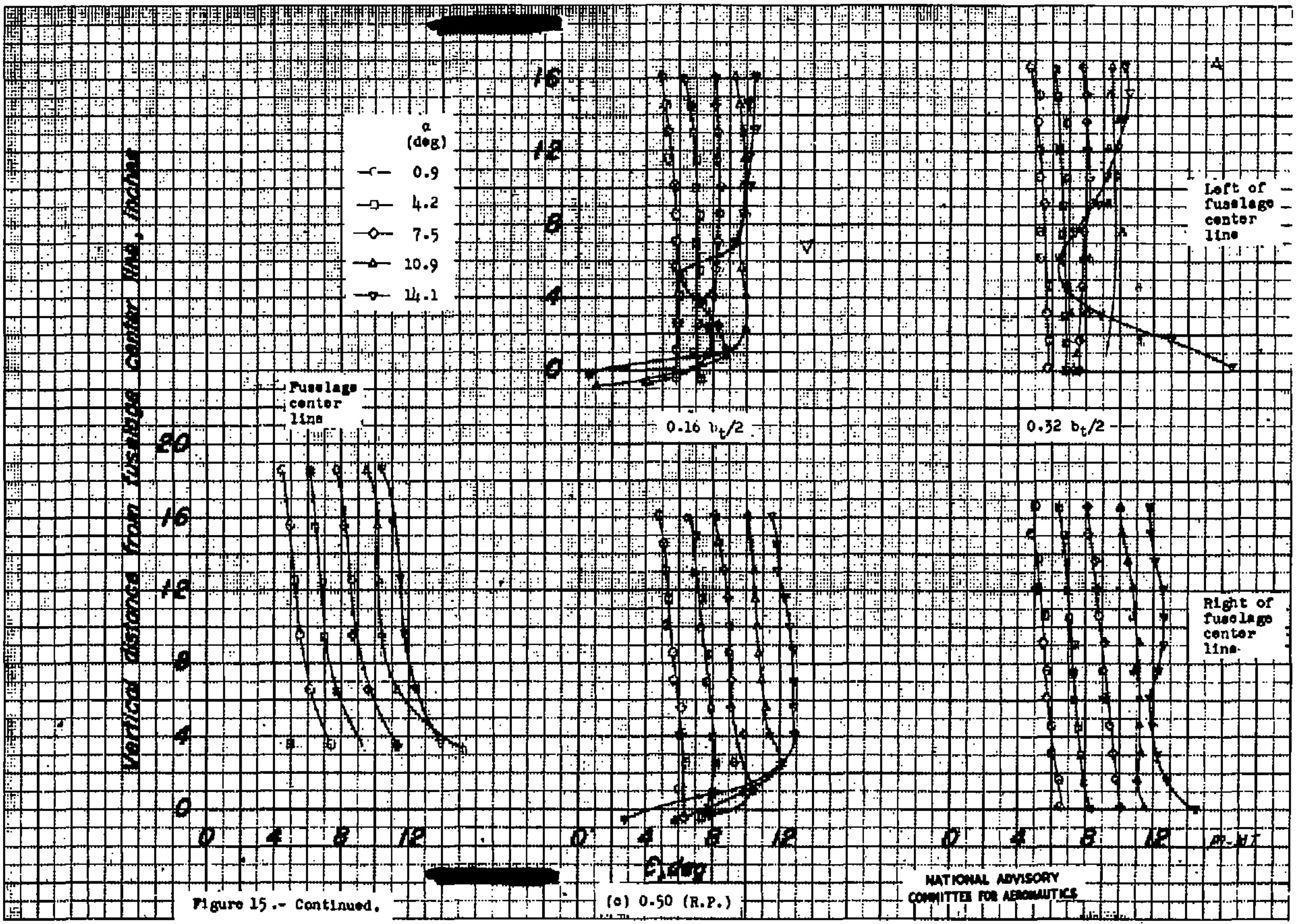

[redacted]

Figure 15.- Continued.

(c) 0.50 (R.P.)

210415

[redacted]

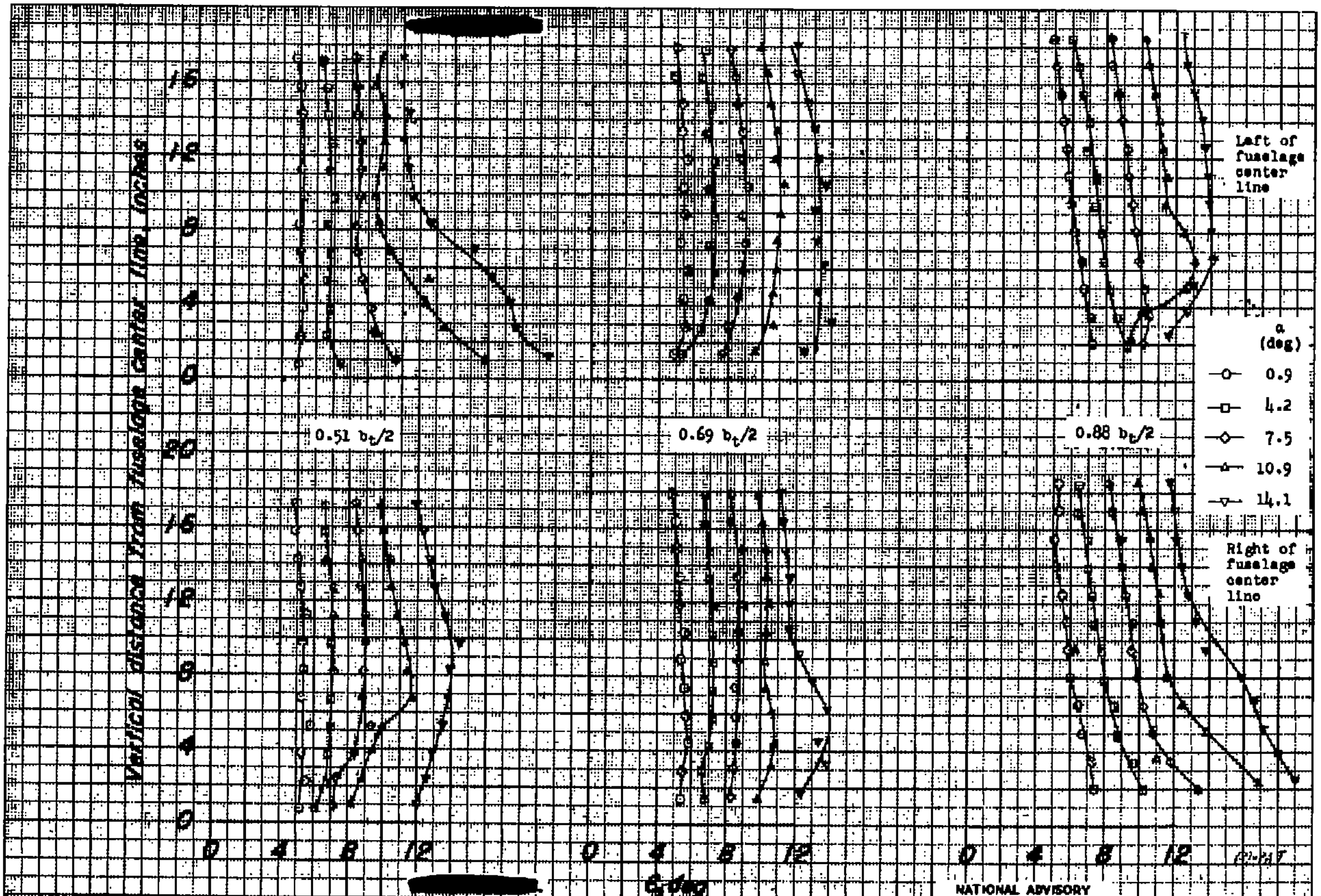

[redacted]

NATIONAL ADVISORY COMMITTEE FOR AERONAUTICS

Figure 15.- Concluded.

(c) Concluded; 0.50 (R.P.)

Fig. 15c conc.